

Towards high partial waves in lattice QCD with an extended two-hadron operator

Jia-Jun Wu¹, Waseem Kamleh,² Derek B. Leinweber², Yan Li,¹ Gerrit Schierholz³,
Ross D. Young,² and James M. Zanotti²

(CSSM-QCDSF Collaboration)

¹*School of Physical Sciences, University of Chinese Academy of Sciences (UCAS), Beijing 100049, China*

²*Special Research Centre for the Subatomic Structure of Matter (CSSM), Department of Physics,
University of Adelaide, Adelaide, South Australia 5005, Australia*

³*Deutsches Elektronen-Synchrotron DESY, Notkestraße 85, 22607 Hamburg, Germany*



(Received 7 September 2021; accepted 22 March 2022; published 22 April 2022)

An extended two-hadron operator is developed to extract the spectra of irreducible representations (irreps) in the finite volume. The irreps of the group for the finite volume system are projected using a coordinate-space operator. The correlation function of this operator is computationally efficient to extract lattice spectra of the specific irrep. In particular, this new formulation only requires propagators to be computed from two distinct source locations, at fixed spatial separation. We perform a proof-of-principle study on a $24^3 \times 48$ lattice volume with $m_\pi \approx 900$ MeV by isolating various spectra of the $\pi\pi$ system with isospin-2 including a range of total momenta and irreps. By applying the Lüscher formalism, the phase shifts of S - and D -wave $\pi\pi$ scattering with isospin-2 are extracted from the spectra, with a tentative look at the role and influence of the G -wave.

DOI: [10.1103/PhysRevD.105.074506](https://doi.org/10.1103/PhysRevD.105.074506)

I. INTRODUCTION

The numerical simulation of quark and gluon fields on a finite lattice enables a study of the hadron spectrum and strong interactions of QCD via first principles. Recently, there has been tremendous progress in lattice QCD calculations of the hadron spectrum and interactions (see Refs. [1–3] for recent reviews). From the energy levels of lattice QCD, there is a clear strategy for how to extract scattering information for two-body systems, such as the $\pi\pi$ system [4–8]. In order to map out the energy dependence of the scattering phase shifts various methods have been developed to access more finite-volume energy levels, such as the variational analysis for the excited-energy eigenvalues [9–12], moving systems [4,6], and twisted boundary conditions [13,14]. An important requirement to isolate distinct partial waves is the need to distinguish the energy levels in different irreducible representations (irreps), such as done in Ref. [6].

With improved control of orbital motion, there is potential for lattice QCD to provide insight into the phenomenology of high-spin systems. For instance, the relatively narrow dibaryon resonance observed by WASA at COSY [15,16] suggests significant coupling to the np G -wave amplitude. There is also potential to shed light on the nuclear $A(y)$ puzzle [17–19] or the dynamics underlying Regge trajectories [20–22]. While each of these objectives will (ultimately) also require advances in many-body systems on the lattice [23,24], the physics of many-body channels can often be suppressed at large unphysical quark masses on the lattice—such as the recent high- J study of Ref. [25].

The study of high angular momentum systems is an ongoing challenge in lattice QCD. On the cubic finite volume of a four-dimensional lattice, the relevant symmetry group is a subgroup of the octahedral group (O_h)—or the relevant little group when considering systems at finite momenta. Importantly, the full $SO(3)$ group of the infinite volume physical theory is broken, and consequently, numerical investigations are limited to the discrete symmetry of the lattice. The issue of partial-wave mixing, and influence on discrete spectra, has been investigated theoretically and numerically in previous work, e.g., Refs. [26–41].

In this paper, we introduce a novel operator construction, designed to provide an efficient method to isolate different

Published by the American Physical Society under the terms of the Creative Commons Attribution 4.0 International license. Further distribution of this work must maintain attribution to the author(s) and the published article's title, journal citation, and DOI. Funded by SCOAP³.

lattice irreps in a two-hadron system. The method relies upon constructing an operator that corresponds to a “dumbbell” in coordinate space, where the two-body operator is the product of two single particle operators separated by a fixed distance. The construction shares similarities with the “cube” source employed in Ref. [37]. In our case, as will be shown, we sum over the rotations of the dumbbell at the sink in order to project correlation functions onto the desired irrep. The two distinguishing features of this method are that only the total momentum of the two-hadron system is fixed and only two point-source Dirac matrix inversions are required. As an exploratory exercise, we study the isospin- $2\pi\pi$ system, for which several alternative methods have already been explored [5–7]. We demonstrate that we are able to successfully determine energy levels of the various representations with different total momenta.

In Sec. II, the two-hadron operator and correlation functions for specific irreps are constructed. In Sec. III, a lattice-QCD calculation for isospin-2 $\pi^-\pi^-$ scattering is presented with lattice size $24^3 \times 48$ and the energy levels for various irreps with different total momentum are extracted. These energy levels are then used to determine the phase shifts of $\pi^-\pi^-$ scattering. Finally, results are summarized in Sec. IV.

II. FORMALISM

A. Operators in coordinate space

Our goal is to construct extended interpolating operators which project onto states of both definite momenta and irreps of the lattice rotation group. To minimize the numerical cost associated with inversion of Dirac matrices, we seek a construction which allows our correlation functions to be constructed from just two conventional local sources. The projection onto definite Fourier momenta and rotational irreps are to be performed at the sink, as depicted in Fig. 1. To construct the appropriate projections we start from a composite operator of two hadrons with a separation δ between them,

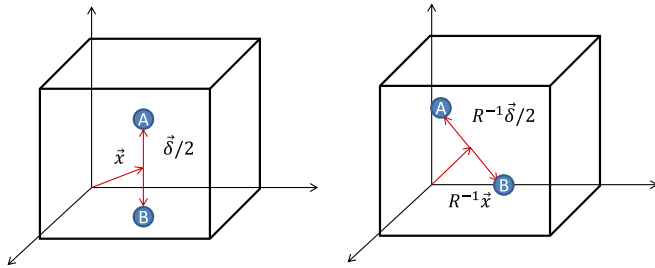


FIG. 1. Illustration of the two-hadron “dumbbell” interpolating operator. Two hadrons named A and B are shown in the cubic box. A fixed source location is indicated in the left image with $\vec{x} + \vec{\delta}/2$ for particle A and $\vec{x} - \vec{\delta}/2$ for particle B. The right panel indicates that the sink operator is to be rotated by a lattice rotation, R , with a weight chosen to project onto the corresponding irrep.

$$\Phi(\mathbf{x}, \delta) \equiv \phi(\mathbf{x} + \delta/2)\phi'(\mathbf{x} - \delta/2), \quad (1)$$

where time dependence has been suppressed and the operator ϕ (or ϕ') denotes a conventional, local single-hadron operator. For example, in the following calculation, we consider the standard π^- operator given by

$$\phi(\mathbf{x}) = \phi'(\mathbf{x}) \equiv \sum_a \bar{u}^a(\mathbf{x})\gamma_5 d^a(\mathbf{x}), \quad (2)$$

with a sum over the color index a .

We consider the set of operators, $\{\Phi_{\hat{R}}\}$, which are related by a lattice rotation, $\hat{R} \in O_h$. Under such a rotation, the transformed operators take the form,

$$\begin{aligned} \Phi_{\hat{R}}(\mathbf{x}, \delta) &\equiv \hat{P}_{\hat{R}}\Phi(\mathbf{x}, \delta)\hat{P}_{\hat{R}^{-1}} = \Phi(\hat{R}^{-1}\mathbf{x}, \hat{R}^{-1}\delta) \\ &= \phi(\hat{R}^{-1}(\mathbf{x} + \delta/2))\phi'(\hat{R}^{-1}(\mathbf{x} - \delta/2)), \end{aligned} \quad (3)$$

as being represented in the right panel of Fig. 1. To maximally span the space of lattice irreps, we choose to work with separation vectors satisfying $0 < \delta_x < \delta_y < \delta_z$ such that $\hat{R}\delta \neq \delta$ (for $\hat{R} \neq I$). We then have 24 different operators that are related by a lattice rotation—in the case of nonidentical particles, there are 48 operators. While the single-hadron operators must lie on lattice sites, the center of the composite operator, \mathbf{x} , need not be on a lattice site. In the numerical results presented here, we work with the choice $\delta = (1, 3, 5)$ and $\mathbf{x} = (1/2, 1/2, 1/2)$. We note that choosing all even values for δ would place the origin of the extended operator on a lattice site and maintain the same discrete rotational symmetries. In principle, combinations of even and odd displacements by δ would be possible, but it would lead to a (short distance) modification of the rotational symmetries discussed here.

A Fourier transform with respect to the coordinate \mathbf{x} project onto states of definite momenta,

$$\langle \Phi(\mathbf{P}, \delta) | = \langle \Omega | \sum_{\mathbf{x}} e^{-i\mathbf{P}\cdot\mathbf{x}} \Phi(\mathbf{x}, \delta). \quad (4)$$

In just the same way that the Fourier transform projects onto states of definite momenta, particular linear combinations of operators related by lattice rotations, Eq. (3), will project onto particular irreducible representations. In particular, for $(|\mathbf{p}|L/2\pi)^2 = 0, 1, 2$, and 3, operators are constructed to project onto the irreps of the groups commonly denoted O_h , C_{4v} , C_{2v} and C_{3v} , respectively (see for instance, Ref. [42]). The projection onto these irreps has been discussed in a number of previous works [4,31,33,34,43]. For completeness and to set our notation, we briefly summarize the relevant features here.

The states $|\Phi_{\hat{R}}(t; \mathbf{x}, \delta)\rangle$ where \hat{R} belong to the corresponding group will transform as vectors of the regular representation as follows:

$$\hat{P}_{\hat{R}}|\Phi_{\hat{R}'}(\mathbf{x}, \delta)\rangle = \sum_{\hat{R}'' \in G^{\mathbf{p}}} |\Phi_{\hat{R}''}(\mathbf{x}, \delta)\rangle (\bar{B}(\hat{R}))_{\hat{R}'', \hat{R}'}, \quad (5)$$

where $(\bar{B}(\hat{R}))_{\hat{R}'', \hat{R}'} = \delta_{\hat{R}\hat{R}'', \hat{R}'}$, and $G^{\mathbf{p}}$ denotes the rotation group for specific total momentum \mathbf{p} (see Table VI).

The regular representation of any nontrivial group is reducible. Thus, \bar{B} can be made block diagonal according to the irreps of the symmetry group via a unitary transformation matrix \bar{S} . For example, in the O_h group,

$$\bar{S}^{-1} \bar{B}(\hat{R}) \bar{S} = 1\bar{A}_1^{\pm}(\hat{R}) \oplus 1\bar{A}_2^{\pm}(\hat{R}) \oplus 2\bar{E}^{\pm}(\hat{R}) \oplus 3\bar{T}_1^{\pm}(\hat{R}) \oplus 3\bar{T}_2^{\pm}(\hat{R}) \equiv \bar{A}(\hat{R}), \quad (6)$$

where $\bar{\Gamma}(\hat{R})$ denotes the representation matrix of \hat{R} in the irrep Γ , and the number before $\bar{\Gamma}$ indicates the number of occurrences of Γ in the regular representation. Using (i, Γ, n) to label the n th vector of the i th occurrence of an irrep Γ , the matrix \bar{A} takes the block diagonal form,

$$\bar{A}_{i\Gamma n, i'\Gamma' n'}(\hat{R}) = \delta_{i'\Gamma' n'} \bar{\Gamma}_{i\Gamma n}(\hat{R}). \quad (7)$$

With the unitary transformation matrix \bar{S} , one can construct the states $|\Psi_{i,\Gamma,n}^{\dagger}\rangle$ as

$$|\Phi_{i,\Gamma,n}^{\dagger}\rangle = \sum_{\hat{R}} |\Phi_{\hat{R}}^{\dagger}\rangle \bar{S}_{R,i\Gamma n}, \quad (8)$$

which will satisfy

$$\hat{P}_{\hat{R}}|\Phi_{i,\Gamma,n}^{\dagger}\rangle = \sum_{i', \Gamma', n'} |\Phi_{i', \Gamma', n'}^{\dagger}\rangle (\bar{A}(\hat{R}))_{i'\Gamma' n', i\Gamma n}. \quad (9)$$

Correspondingly, a new type of two-hadron operator can be defined as in Eq. (A6) as

$$\Phi_{i,\Gamma,n}^{\dagger} = \sum_{\hat{R}} \Phi_{\hat{R}}^{\dagger} \bar{S}_{R,i\Gamma n}. \quad (10)$$

B. Correlation function

The elementary two-point correlation function is constructed from $\Phi_{\hat{R}}(t; \mathbf{x}, \delta)$ at the source and sink as follows:

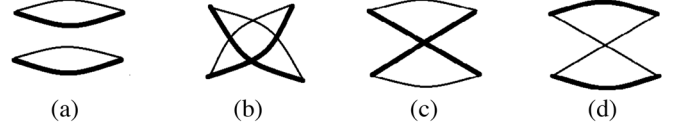


FIG. 2. Diagrams for Wick contractions. Thick and thin lines are to distinguish d and u propagators, respectively.

$$G_{\hat{R}, \hat{R}'}(t; \mathbf{p}; \mathbf{x}, \delta) = \sum_{(\mathbf{y}-\mathbf{x}) \in \mathbb{Z}^3} e^{-i\mathbf{p} \cdot (\mathbf{y}-\mathbf{x})} \times \langle T(\Phi_{\hat{R}}(t; \mathbf{y}, \delta), \Phi_{\hat{R}'}^{\dagger}(0; \mathbf{x}, \delta)) \rangle,$$

where the angle brackets denote the ensemble average across gauge ensembles and T the time-ordered product of field operators. While this generally involves the full set of rotations at source and sink, we can exploit the translational and rotational symmetry of this correlator to obtain,

$$G_{\hat{R}, \hat{R}'}(t; \mathbf{p}; \mathbf{x}, \delta) = G_{\hat{R}\hat{R}^{-1}, \hat{I}}(t; \mathbf{p}; \mathbf{x}, \delta) \quad \forall \hat{R}, \hat{R}' \in G^{\mathbf{p}}. \quad (11)$$

The projection of the correlation function onto definite irreps of the lattice rotation group is then given by

$$\tilde{G}_{\Gamma}(t; \mathbf{p}; \mathbf{x}, \delta) = \sum_{(\mathbf{y}-\mathbf{x}) \in \mathbb{Z}^3} e^{-i\mathbf{p} \cdot (\mathbf{y}-\mathbf{x})} \sum_i \langle T(\Phi_{i,\Gamma,n}(t; \mathbf{y}, \delta), \Phi_{i,\Gamma,n}^{\dagger}(0; \mathbf{x}, \delta)) \rangle \quad (12)$$

$$= \sum_{\hat{R}} \chi_{\hat{R}}^{\Gamma} G_{\hat{R}, \hat{I}}(t; \mathbf{p}; \mathbf{x}, \delta), \quad (13)$$

where $\chi_{\hat{R}}^{\Gamma}$ is the character number of element \hat{R} of the group in the irrep Γ . See Appendix A for an in depth discussion.

A demonstration of the technique introduced here is performed in the $\pi^{-}\pi^{-}$ system. The individual contributions, $G_{\hat{R}^{-1}, \hat{I}}$, to the target correlation functions are given in terms of the Wick contractions shown in Fig. 2, given explicitly by

$$\begin{aligned} G_{\hat{R}^{-1}, \hat{I}}(t; \mathbf{p}; \mathbf{x}, \delta) = & \sum_{(\mathbf{y}-\mathbf{x}) \in \mathbb{Z}^3} e^{i\mathbf{p} \cdot (\mathbf{y}-\mathbf{x})} \{ \text{Tr}[S_d(\mathbf{y}_R^-, t; \mathbf{x}^-) S_u^{\dagger}(\mathbf{y}_R^-, t; \mathbf{x}^-, 0)] \text{Tr}[S_d(\mathbf{y}_R^+, t; \mathbf{x}^+, 0) S_u^{\dagger}(\mathbf{y}_R^+, t; \mathbf{x}^+, 0)] \\ & + \text{Tr}[S_d(\mathbf{y}_R^+, t; \mathbf{x}^-, 0) S_u^{\dagger}(\mathbf{y}_R^+, t; \mathbf{x}^-, 0)] \text{Tr}[S_d(\mathbf{y}_R^-, t; \mathbf{x}^+, 0) S_u^{\dagger}(\mathbf{y}_R^-, t; \mathbf{x}^+, 0)] \\ & - \text{Tr}[S_d(\mathbf{y}_R^-, t; \mathbf{x}^-, 0) S_u^{\dagger}(\mathbf{y}_R^+, t; \mathbf{x}^-, 0) S_d(\mathbf{y}_R^+, t; \mathbf{x}^+, 0) S_u^{\dagger}(\mathbf{y}_R^-, t; \mathbf{x}^+, 0)] \\ & - \text{Tr}[S_d(\mathbf{y}_R^+, t; \mathbf{x}^-, 0) S_u^{\dagger}(\mathbf{y}_R^-, t; \mathbf{x}^-, 0) S_d(\mathbf{y}_R^-, t; \mathbf{x}^+, 0) S_u^{\dagger}(\mathbf{y}_R^+, t; \mathbf{x}^+, 0)] \}. \end{aligned} \quad (14)$$

Here we have made use of the notation

$$\mathbf{x}^\pm = \frac{2\mathbf{x} \pm \boldsymbol{\delta}}{2}, \quad \mathbf{y}_R^\pm = \frac{2\mathbf{y} \pm \hat{R}\boldsymbol{\delta}}{2}, \quad (15)$$

and $S_q(\mathbf{y}, t; \mathbf{x}, 0)$ denotes a conventional point-to-all propagator. The quark flavors, $q = u$ or d , are shown explicitly, however in the following numerical calculation we assume isospin symmetry, $S_u = S_d$.

Given the form of the correlator construction, we note that the correlation function can be efficiently calculated by only performing Dirac matrix inversions from two distinct sites \mathbf{x}^\pm . Furthermore, in the moving frame, the same spectra are extracted from the set of $\tilde{G}_\Gamma(t; \mathbf{p}; \mathbf{x}, \boldsymbol{\delta})$ with the same $|\mathbf{p}|$. One can therefore sum over each direction to reduce the statistical variance, i.e.,

$$\tilde{G}_\Gamma(t; P; \mathbf{x}, \boldsymbol{\delta}) = \sum_{\mathbf{p}, |\mathbf{p}|=P} \sum_{\hat{R} \in G^{\mathbf{p}}} \chi_{\hat{R}}^\Gamma G_{\hat{R}, \hat{I}}(t; \mathbf{p}; \mathbf{x}, \boldsymbol{\delta}), \quad (16)$$

where, as above, $G^{\mathbf{p}}$ denotes the rotation group for specific total momentum \mathbf{p} .

In the following section we present numerical results for the determination of the ground states in each of the considered irreps up to $P^2 = 3P_0^2$, where P_0 defines the basic momentum unit in the box $P_0 \equiv 2\pi/L$.

III. NUMERICAL RESULTS

A. Lattice setup

Following the prescription given by Eqs. (14) and (16) and Tables V and VI, the correlation functions of the $\pi^- \pi^-$ system are analyzed for various total momenta and irreps of the lattice rotation group. The present calculation is performed on an ensemble with two flavors of dynamical $\mathcal{O}(a)$ -improved Wilson fermions with $\beta = 5.29$, $\kappa = 0.13550$ on a $24^3 \times 48$ volume, corresponding to $a = 0.071$ fm and $m_\pi \simeq 900$ MeV, from the QCDSF Collaboration [44].

Results are collected from 376 configurations using 16 different randomized source locations, totalling $\mathcal{O}(6,000)$ measurements. With two distinct propagators required for each source, the comparative computational cost of the present calculation is $\mathcal{O}(12,000)$ measurements.

B. Spectra

In this study, we consider correlation functions with total momentum up to three lattice units $|\mathbf{p}| \leq \sqrt{3}P_0$. The correlation functions for each irrep are fit with a parametrization taking the form,

$$G(t) = A(e^{-Et} + e^{-E(T-t)}) + B(e^{-\Delta Et} + e^{-\Delta E(T-t)}), \quad (17)$$

where the fit parameters A and E correspond to the amplitude and two-point energy of interest. The term

involving B is provided to isolate the leading contribution arising from thermal states, as is familiar in studies of multihadron correlators [6,45–50]. For the present study, this corresponds to one pion propagating forwards and the other backwards in Euclidean time. The value of the exponent in the thermal contribution is held fixed to $\Delta E = E_\pi(\mathbf{p} - \mathbf{k}) - E_\pi(\mathbf{k})$, for single-pion energies E_π , and \mathbf{k} chosen to correspond to the lightest single pion state contributing to the given correlator. At large temporal extent, the coefficient B should scale according to $e^{-E_\pi(\mathbf{k})T}$. While we don't have numerical results at different T , we see that the fitted values of B are always suppressed by this order of magnitude compared to A .

After subtracting the contributions from thermal states, Fig. 3 displays the effective mass for different total momenta and irreducible representation. We see a clear separation of the energy levels in distinct irreps. As expected, the low-lying A_1 irreps are generally cleaner statistically, whereas the signal quality degrades for the irreps corresponding to the resolution of higher-spin partial waves.

The results for the extracted energy levels are shown by the black circles in Fig. 4. For comparison, the low-lying noninteracting energy levels in each system are displayed by the grey lines. Each of the energy levels isolated are consistent with some degree of weak repulsion, as expected for the $I = 2$ state. For most of the states considered, the first excited state is expected to be clearly separated, and hence the ground-state isolation should be reliable (to within the statistical uncertainties of this work). However, there are three particular channels where multiple low-lying states are anticipated, arising from the clustering of noninteracting two-particle energy levels. These include

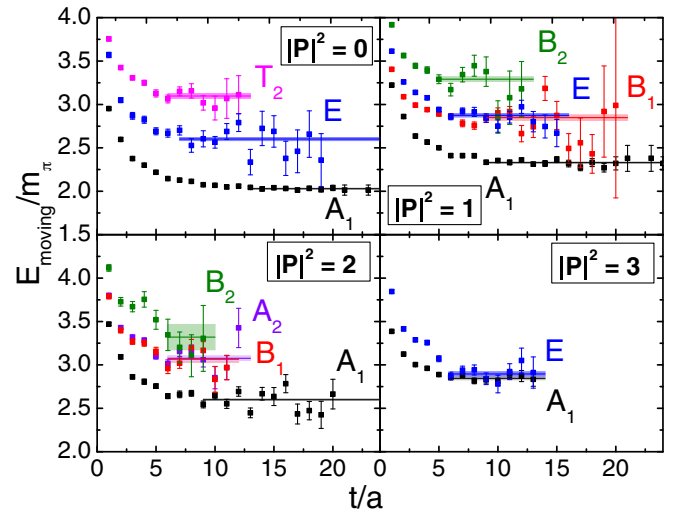


FIG. 3. The effective energies for different total momenta P (in multiples of $2\pi/L$), and different irreps. The bands display the two-pion energies fitted to Eq. (17). The horizontal width of the bands indicates the corresponding fit window.

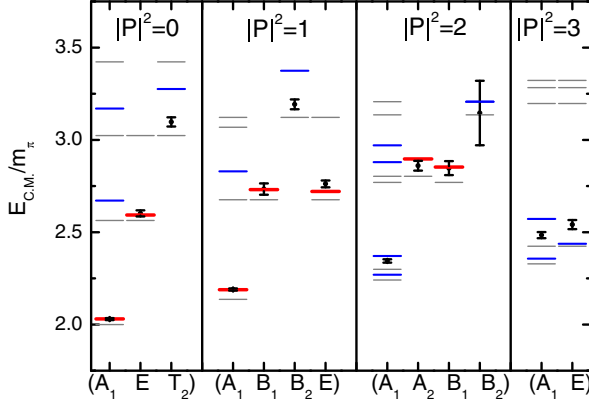


FIG. 4. The energy levels of the various systems with different total momenta and irreps. The black points show the extracted center-of-momentum (CM) energies. The grey lines display the locations of the corresponding noninteracting energies. The red lines show the fitted energies according to fit (iii), as described in Table II, and the blue lines display further predicted eigenvalues based upon this fit.

A_1 at $P^2 = 2P_0^2$, $3P_0^2$ and B_2 at $P^2 = 2P_0^2$. In these cases, we do not expect that our correlation functions are dominated by a single ground-state energy and hence the fitted parameters are not representative of eigenenergies of the system.

Within the operator construction presented, only the total momentum is specified, whereas the momentum of each pion is not. In contrast to Refs. [7,37], which involve momentum-projected hadrons at the sink, we use the same operators at both the source and sink. While staying within the paradigm of local sources, this method then lends itself to a variational analysis [11,51,52], where the operator basis can be extended by varying $|\delta|$.

C. Phase shifts

We use the following Lüscher formula [5,26,31], assuming that exponentially-suppressed corrections can be neglected, to extract phase shifts from finite-volume spectra,

$$\det[M_{\ell n, \ell' n'}^{\Gamma, \mathbf{p}}(q(\Gamma)) - \delta_{\ell, \ell'} \delta_{n, n'} \cot \delta_\ell(q(\Gamma))] = 0. \quad (18)$$

The matrix $M_{\ell n, \ell' n'}^{\Gamma, \mathbf{p}}$ has been discussed extensively in the literature, see e.g., Refs. [28,31,34]. For completeness, we provide detail relevant to the present investigation in the Appendix B.

As encoded by Eq. (18), each energy level determined on the lattice is constrained by multiple partial waves—see Table I. This necessitates the use of a parametrization of the energy dependence of the phase shifts in order to isolate the individual partial waves. For the purpose of this investigation, we consider the parametrization of the ℓ -wave phase shifts by the effective range expansion,

TABLE I. The relationship between angular momentum and irrep in the various momentum. The total angular momentum quantum number for exact spherical symmetry are only quoted up to $\ell = 4$.

Group	$ \mathbf{p}L/2\pi ^2$	Γ	ℓ
O_h	0	A_1^+	0, 4
		A_2^+	>4
		E^+	2, 4
		T_1^+	4
		T_2^+	2, 4
C_{4v}	1	A_1	0, 2, 4
		A_2	>4
		B_1	2, 4
		B_2	2, 4
		E	2, 4
C_{2v}	2	A_1	0, 2, 4
		A_2	2, 4
		B_1	2, 4
		B_2	2, 4
		E	2, 4
C_{3v}	3	A_1	0, 2, 4
		A_2	>4
		E	2, 4

$$q^{2\ell+1} \cot \delta_\ell = \frac{1}{a_\ell} + \frac{1}{2} r_\ell q^2, \quad (19)$$

for parameters a_ℓ and r_ℓ —for $\ell = 0$ these are familiarly recognized as the scattering length and effective range, respectively. Such a parametrization should be reasonable for the weakly-repulsive interactions anticipated in $I = 2$ scattering.

As described above, we do not expect that our extracted energy levels in A_1 at $P^2 = 2P_0^2$, $3P_0^2$, or B_2 at $P^2 = 2P_0^2$ are meaningful representations of an energy eigenstate, and hence these are excluded from any fits. This leaves up to ten data points for constraining the phase shift parametrization. We summarize the various fit forms and corresponding results in Tables II and III, respectively. In the following we provide a description of each scenario considered:

TABLE II. Summary of the various fit strategies that have been included, as detailed in the text. The first column indicates the presence of the isolated eigenstate for the E irrep at $P^2 = 3P_0^2$. The second column denotes a truncation of the dataset at center-of-mass energies of $3m$. The corresponding number of data points is given by N_{data} . To the right of the vertical divide line, we show the included fit parameters from Eq. (19).

Fit	$\{3E\}$	$\{E^*/m > 3\}$	N_{data}	$a_{0,2}$	a_4	r_0	r_2
I	✓	✓	10	✓	✓	✗	✗
II	✗	✓	9	✓	✓	✗	✗
III	✗	✓	9	✓	✓	✓	✗
IV	✗	✓	9	✓	✓	✗	✓
V	✗	✗	7	✓	✓	✗	✗
VI	✗	✗	7	✓	✗	✗	✗

TABLE III. Best fit parameters for different fits, as described in the text and summarized in Table II. The final two columns indicate the total and reduced χ^2 values, respectively.

Fit	a_0	r_0	a_2	$r_2 \times 10^6$	a_4	χ^2	χ_r^2
I	-0.690(53)	...	-0.0111(84)	...	-0.0200(41)	36.2	5.2
II	-0.691(65)	...	-0.0092(64)	...	-0.0208(43)	15.5	2.6
III	-0.65(11)	0.7(19)	-0.0091(90)	...	-0.0208(67)	15.4	3.1
IV	-0.691(53)	...	-0.0092(96)	0.5(51)	-0.0208(67)	15.5	3.9
V	-0.683(65)	...	-0.0602(58)	...	-0.0118(48)	7.2	1.8
VI	-0.678(47)	...	-0.0871(26)	9.6	1.9

- Fit (i) We include all 10 viable data points with a simple leading-order parameter a_ℓ in each partial wave.
- Fit (ii) In Fit (i), we find that the E representation at $P^2 = 3P_0^2$ is incompatible with the fit form, as shown in Table III, and hence we drop this point from this and subsequent fits. Dropping this one point improves the reduced χ^2 (χ_r^2) significantly, yet still suggests some tension with the data.
- Fit (iii) This is as in Fit (ii), with an r_0 parameter also included. The parameter r_0 is poorly determined, and the reduced χ^2 increases significantly.
- Fit (iv) This is as in Fit (ii), with an r_2 parameter included. Similar to Fit (iii), r_2 is poorly determined, and the reduced χ^2 increases significantly.
- Fit (v) We further restrict the fits to only consider the lowest-lying center-of-mass energies, where both the effective range expansion, and truncation of partial waves in the quantization condition are expected to be most reliable. Specifically, we choose $E_{\text{CM}} < 3m_\pi$ and fit the three parameters $a_{0,2,4}$. The fit quality is reasonable, although still may point to some mild tension with the underlying lattice results.

- Fit (vi) This is the same as Fit (v), but with just two parameters, $a_{0,2}$. Evidently, the removal of a_4 does not appreciably degrade the fit quality.

We consider that Fits (v) and (vi) are equally good fits of the lattice spectra. We show the parametrizations from each of these fits in the two panels of Fig. 5. Considering the negligible difference in the quality of the corresponding χ^2 , there is no clear signal for an interaction in the G -wave channel. However, it is interesting to note that the extracted $\ell = 2$ interaction, by way of the parameter a_2 , is sensitive to the inclusion or not of the $\ell = 4$ partial wave.

It is interesting to examine the individual point-by-point extractions of the phase shifts. In particular, if we neglect the $\ell \geq 4$ interactions, we have a simple one-to-one mapping between most of the lattice eigenstates and the corresponding phase shifts. In the left panel of Fig. 5, the black data points indicate these direct phase shift extractions, under the assumption of negligible $\ell = 4$ interactions. The A_1 irrep at $|P|^2 = P_0^2$ mixes $\ell = 0$ and 2, as seen in Table I, and hence the eigenvalue equation ultimately provides a single constraint between the two corresponding phase shifts. The data points displayed, shown in open pink symbols, indicate the extraction of

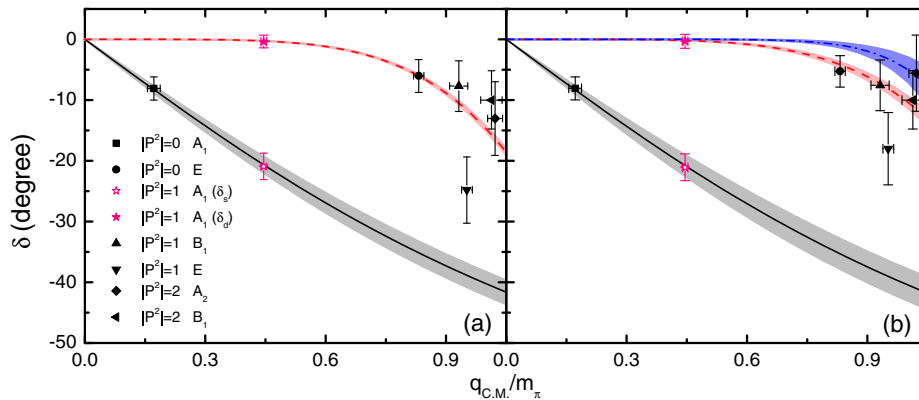


FIG. 5. The phase shifts from Fits (vi) and (v) are illustrated in (a) and (b), respectively. The solid black, dashed red, and dash-dotted blue curves are for the S -, D -, and G -wave phase shifts. Each of the black data points display the phase shifts directly solved for from the individual energy levels, where the G -wave is taken to vanish (a) or given by the corresponding parametrization of Fit (v) (b). Furthermore, the open pink points are the phase shifts of S - and D -wave for A_1 irrep of $|P|^2 = P_0^2$ which are determined using the corresponding fit for δ_2 and δ_0 , respectively.

δ_0 (δ_2) using the parametrization for δ_2 (δ_0) from Fit (vi). The right panel of Fig. 5 shows a similar pointwise extraction of the phase shifts, where $\delta_{0,2}$ are presented under the assumption of δ_4 from Fit (v). We see that the S -wave (being at lower energies) is completely insensitive to the presence of δ_4 , however the δ_2 phase shifts do exhibit a small realignment.

The sensitivity of the $\ell = 2$ phase shifts to the presence of $\ell = 4$ is therefore revealed in both the global parametrizations and the pointwise analysis. While evident that the $\ell = 2$ partial wave is dominating the quantization condition, it is interesting to note that the systematic uncertainty in δ_2 from the partial wave truncation is dominant over the corresponding statistical uncertainty.

Finally, we note that the a_2 parameter is quite small in Fits (i) to (iv), in exchange for a relatively large a_4 . Given that the corresponding fits appear to be a poor representation of the corresponding energy eigenstates, we do not attempt an interpretation of these small a_2 values.

D. Discussion

We compare the statistical precision obtained with other calculations of the isospin- $2\pi\pi$ system in lattice QCD. The level of statistics span a broad range, and the needs can vary dramatically depending on the complexity of the target observables. For reference on the scale of the computations, we compare $\mathcal{O}(4,500)$ fermion-matrix inversions by NPLQCD to extract the S -wave scattering length [53]; $\mathcal{O}(290,000)$ by NPLQCD [54] for the energy-dependent S -wave phase shifts [7]; and $\mathcal{O}(270,000)$ by Dudek *et al.* to isolate S - and D -wave phase shifts [6]. To provide guidance on the relative precision, we note that our relative error of scattering length of S -wave is around 10%, while it is $\sim 2\%$ in Ref. [6], thus the accuracy could be considered comparable after accounting for a factor of $\mathcal{O}(20)$ difference in counting statistics. We caution taking too much from this comparison. Systematic effects can evolve as statistical precision increases, and certainly the calculation of Dudek *et al.* was set up to consider systems at different isospin, which are not available in the present work.

We note that the present method could be extended to consider systems involving quark propagators from one time slice back onto itself, such as required for $I = 0$ and $1 \pi\pi$ scattering. While the present dumbbell formulation is envisaged for application in baryon-baryon scattering, where such diagrams are not present, it could be interesting to apply this to more general systems, where loop propagators present unique challenges.

In the context of baryon-baryon systems, we note that a key feature of the construction is that one can make use of variational techniques—something that is unavailable with more standard point-to-Fourier correlators. Extending the operator basis to span a greater range of δ values does require having more single-site inversions at each source time slice. In principle, this does come at additional cost in

terms of the number of propagators calculated. In the present study, we accumulated statistics with 16 random sources on each configuration, corresponding to 32 single-site inversions. If all these inversions were to be done from a single time slice, one could design the locations appropriately to span a range of delta values without any significant increase in the overall computational cost. Thus, in future work, there is the possibility to exploit the combinatorial gain in having (up to) $N(N-1)/2$ pairwise separations for N inversion sites.

IV. SUMMARY AND OUTLOOK

In this paper, we introduce a new extended operator to extract the spectra of irreducible representations at rest and in moving systems. In coordinate space, the two-particle operator projects onto an irrep by summing appropriately over a spherical shell. The method is straightforward to implement as a generalization of conventional point sources, and hence offers an alternative for cases where stochastic momentum sources are impractical.

For the numerical investigation in this work, we studied the isospin- $2\pi\pi$ system at a range of total momenta, on a $24^3 \times 48$ volume with a lattice spacing of $a = 0.071$ fm and $m_\pi \approx 900$ MeV. The correlation functions of various irreps with a total momentum-squared ranging from 0 to 3 have been studied, with 13 plateaus—10 of which were considered as viable ground-state candidates. These discrete finite volume spectra have then been analyzed with the Lüscher quantization condition. Using a simple effective range expansion of the phase shifts, we identify S - and D -wave interactions, and a tentative first look at G -wave contributions.

In the future, this method can also be readily extended to particles with spin, particularly for the two baryon system. Including a basis of operators at different hadronic separations would allow for a variational analysis to be performed, and thereby allow for a determination of the excited energy levels on the lattice. This would correspond to an analog of mapping out the quantum mechanical coordinate space-wave function.

ACKNOWLEDGMENTS

The calculations presented in this manuscript made use of the Chroma software library [55]. This research was supported with supercomputing resources provided by the Phoenix HPC service at the University of Adelaide and the National Computational Infrastructure (NCI). NCI resources were provided through the National Computational Merit Allocation Scheme, supported by the Australian Government through Grants No. LE160100051 and No. LE190100021 (D.B.L. and J.M.Z.) and the University of Adelaide Partner Share. This investigation has been supported by the Australian Research Council under Grants No. DP140103067 (R.D.Y., J.M.Z. and

D. B. L.), No. DP190100297 (J. M. Z. and R. D. Y.), No. DP190102215 (D. B. L.), and No. DP210103706 (D. B. L.). G. S. was supported by DFG Grant No. SCHI 179/8-1. J. J. W. was supported by the Fundamental Research Funds for the Central Universities and National Key R&D Program of China under Contract No. 2020YF A0406400.

APPENDIX A: OCTAHEDRAL GROUP (O_h) AND ITS LITTLE GROUPS

1. The 48 elements of O_h group

The cubic group (O) has 24 elements indicated as R_i ($i = 1-24$) which correspond to 24 rotations, \hat{R}_i as listed in Table IV. Starting with one vector $\delta_1 \equiv (q_1, q_2, q_3)$, one can then construct 23 vectors via \hat{R}_i ($i = 2-24$) (\hat{R}_1 is the identity operator) as follows:

$$\delta_i = \hat{R}_i \delta_1, \quad (A1)$$

In Table IV, the 24 vectors δ_i are all listed. The O_h group can be recognized as the product of the O group and the $C_2 = \{e, \hat{\sigma}\}$ group, i.e., $O_h = O \otimes C_2$. Then the other 24 operators belonging to O_h group rather than O group will be $\hat{R}_{i+24} = \hat{\sigma} \hat{R}_i$, and correspondingly, $\delta_{i+24} = -\delta_i$.

TABLE IV. For the O group, 24 vectors δ_i and operators R_i ($i = 1-24$) are listed. $\delta_1^\top \equiv (q_1, q_2, q_3)$ and $R_1 \equiv E$ which is the identity. R_i includes the rotation axis and angle.

Class	R_i	Axis-angle	Euler angle	δ_i^\top
E	R_1	Any 0°	$(0^\circ, 0^\circ, 0^\circ)$	(q_1, q_2, q_3)
$8C'_3$	R_2	$(1, 1, 1) - 120^\circ$	$(90^\circ, 90^\circ, 180^\circ)$	(q_2, q_3, q_1)
	R_3	$(1, 1, 1) + 120^\circ$	$(0^\circ, 90^\circ, 90^\circ)$	(q_3, q_1, q_2)
	R_4	$(-1, 1, 1) - 120^\circ$	$(180^\circ, 90^\circ, 90^\circ)$	$(-q_3, -q_1, q_2)$
	R_5	$(-1, 1, 1) + 120^\circ$	$(90^\circ, 90^\circ, 0^\circ)$	$(-q_2, q_3, -q_1)$
	R_6	$(-1, -1, 1) - 120^\circ$	$(-90^\circ, 90^\circ, 0^\circ)$	$(q_2, -q_3, -q_1)$
	R_7	$(-1, -1, 1) + 120^\circ$	$(180^\circ, 90^\circ, -90^\circ)$	$(-q_3, q_1, -q_2)$
	R_8	$(1, -1, 1) - 120^\circ$	$(0^\circ, 90^\circ, -90^\circ)$	$(q_3, -q_1, -q_2)$
	R_9	$(1, -1, 1) + 120^\circ$	$(-90^\circ, 90^\circ, 180^\circ)$	$(-q_2, -q_3, q_1)$
$6C_4$	R_{10}	$(1, 0, 0) - 90^\circ$	$(90^\circ, 90^\circ, -90^\circ)$	$(q_1, q_3, -q_2)$
	R_{11}	$(1, 0, 0) + 90^\circ$	$(-90^\circ, 90^\circ, 90^\circ)$	$(q_1, -q_3, q_2)$
	R_{12}	$(0, 1, 0) - 90^\circ$	$(180^\circ, 90^\circ, 180^\circ)$	$(-q_3, q_2, q_1)$
	R_{13}	$(0, 1, 0) + 90^\circ$	$(0^\circ, 90^\circ, 0^\circ)$	$(q_3, q_2, -q_1)$
	R_{14}	$(0, 0, 1) - 90^\circ$	$(-90^\circ, 0^\circ, 0^\circ)$	$(q_2, -q_1, q_3)$
	R_{15}	$(0, 0, 1) + 90^\circ$	$(90^\circ, 0^\circ, 0^\circ)$	$(-q_2, q_1, q_3)$
	R_{16}	$(0, 1, 1) - 180^\circ$	$(90^\circ, 90^\circ, 90^\circ)$	$(-q_1, q_3, q_2)$
	R_{17}	$(0, -1, 1) - 180^\circ$	$(-90^\circ, 90^\circ, -90^\circ)$	$(-q_1, -q_3, -q_2)$
$6C'_2$	R_{18}	$(1, 1, 0) - 180^\circ$	$(-90^\circ, 180^\circ, 0^\circ)$	$(q_2, q_1, -q_3)$
	R_{19}	$(1, -1, 0) - 180^\circ$	$(90^\circ, 180^\circ, 0^\circ)$	$(-q_2, -q_1, -q_3)$
	R_{20}	$(1, 0, 1) - 180^\circ$	$(0^\circ, 90^\circ, 180^\circ)$	$(q_3, -q_2, q_1)$
	R_{21}	$(-1, 0, 1) - 180^\circ$	$(180^\circ, 90^\circ, 0^\circ)$	$(-q_3, -q_2, -q_1)$
	R_{22}	$(1, 0, 0) - 180^\circ$	$(180^\circ, 180^\circ, 0^\circ)$	$(q_1, -q_2, -q_3)$
	R_{23}	$(0, 1, 0) - 180^\circ$	$(0^\circ, 180^\circ, 0^\circ)$	$(-q_1, q_2, -q_3)$
	R_{24}	$(0, 0, 1) - 180^\circ$	$(180^\circ, 0^\circ, 0^\circ)$	$(-q_1, -q_2, q_3)$

2. The classes and irreps of O_h group

There are 48 elements in the O_h group and they can be partitioned into ten different classes. There are ten irreps, $A_1^\pm(1)$, $A_2^\pm(1)$, $E^\pm(2)$, $T_1^\pm(3)$, and $T_2^\pm(3)$, where the numbers in the parentheses are the dimensions of these irreps. The character table of the cubic group is shown in Table V.

3. Regular representation

Using the O_h group, a scalar function $\phi(\delta)$ can be extended to 48 functions as follows:

$$\phi_R(\delta) = \hat{P}_R \phi(\delta) = \phi(\hat{R}^{-1} \delta). \quad (A2)$$

Under the group action, they should transform as

$$\begin{aligned} \hat{P}_R \phi_{R'}(\delta) &= \sum_{R''} \phi_{R''}(\delta) (\bar{B}(\hat{R}))_{R'', R} = \hat{P}_R \hat{P}_{R'} \phi(\delta) \\ &= \hat{P}_{RR'} \phi(\delta) = \phi(\hat{R}'^{-1} \hat{R}^{-1} \delta) = \phi_{RR'}(\delta). \end{aligned}$$

Here $\bar{B}(\hat{R})$ is the representation matrix of \hat{R} for the regular representation. The dimension of the regular representation is the same as the order of the group.

TABLE V. Character table of O_h , C_{4v} , C_{2v} and C_{3v} for $|\mathbf{p}L/2\pi|^2 = 0, 1, 2$, and 3, respectively.

O_h	Γ/Class	I	$8C'_3$	$6C_4$	$6C'_4$	$3C_4^2$	$\hat{\pi}$	$8C'_3 \times \hat{\pi}$	$6C_4 \times \hat{\pi}$	$6C'_4 \times \hat{\pi}$	$3C_4^2 \times \hat{\pi}$
	A_1^\pm	1	1	1	1	1	± 1	± 1	± 1	± 1	± 1
	A_2^\pm	1	1	-1	-1	1	± 1	± 1	∓ 1	∓ 1	± 1
	E^\pm	2	-1	0	0	2	± 2	∓ 1	0	0	± 2
	T_1^\pm	3	0	-1	1	-1	± 3	0	∓ 1	± 1	∓ 1
	T_2^\pm	3	0	1	-1	-1	± 3	0	± 1	∓ 1	∓ 1
$C_{4\nu}$	Γ/Class	I	$2C_4$	$2C'_2 \times \hat{\pi}$	$2C_2 \times \hat{\pi}$	C_2					
	A_1	1	1	1	1	1					
	A_2	1	1	-1	-1	1					
	B_1	1	-1	-1	1	1					
	B_2	1	-1	1	-1	1					
	E	2	0	0	0	-2					
$C_{2\nu}$	Γ/Class	I	C'_2	$C'_2 \times \hat{\pi}$	$C_2 \times \hat{\pi}$						
	A_1	1	1	1	1						
	A_2	1	1	-1	-1						
	B_1	1	-1	1	-1						
	B_2	1	-1	-1	1						
$C_{3\nu}$	Γ/Class	I	$2C_3$	$3C'_2 \times \hat{\pi}$							
	A_1	1	1	1							
	A_2	1	1	-1							
	E	2	-1	0							

4. From regular representation to irreps

The regular representation of any nontrivial group is reducible. So \bar{B} can be made block diagonal according to the irreps of O_h via a unitary transformation matrix \bar{S} as follows:

$$\bar{S}^{-1} \bar{B}(\hat{R}) \bar{S} = 1\bar{A}_1^\pm(\hat{R}) \oplus 1\bar{A}_2^\pm(\hat{R}) \oplus 2\bar{E}^\pm(\hat{R}) \oplus 3\bar{T}_1^\pm(\hat{R}) \oplus 3\bar{T}_2^\pm(\hat{R}) \equiv \bar{A}(\hat{R}). \quad (\text{A3})$$

The number before the irrep indicates the occurrence of that irrep. At last you will find $48 = 2(1^2 + 1^2 + 2^2 + 3^2 + 3^2)$. And the matrix \bar{A} can be written as

$$\bar{A}_{i\Gamma n, i'\Gamma' n'}(\hat{R}) = \delta_{i'i} \delta_{\Gamma'\Gamma} \bar{\Gamma}_{n, n'}(\hat{R}), \quad (\text{A4})$$

where Γ is the name of the irrep, and i shows how many times it appears, for example $i = 1, 2, 3$ for T_1^\pm and T_2^\pm , and $i = 1, 2$ for E , and $i = 1$ for A_1^\pm and A_2^\pm ; and n indicates the order of the irrep Γ . The matrix $\bar{\Gamma}(\hat{R})$ is the matrix representation of element \hat{R} in the irrep Γ . Because O_h is a finite group, the matrices $\bar{\Gamma}$ can be chosen to be unitary.

As shown in Eq. (A3), the matrices $\bar{B}(\hat{R})$ show the rotations of 48 scalar functions ϕ . Then matrices \bar{A} also have 48 scalar functions satisfying,

$$\hat{P}_R \Phi_{i\Gamma, n}(\delta) = \sum_{i', \Gamma', n'} \Phi_{i', \Gamma', n'}(\delta) (\bar{A}(\hat{R}))_{i'\Gamma' n', i\Gamma n}. \quad (\text{A5})$$

The transformation matrix \bar{S} can connect Φ_R and $\Phi_{i\Gamma, n}$ as follows:

$$\Phi_{i\Gamma, n} = \sum_R \phi_R \bar{S}_{R, i\Gamma n}. \quad (\text{A6})$$

The row index of \bar{S} is the name of the elements of the cubic group, and the column index is the same as the indices of Φ , (i, Γ, n) .

On the other hand, from Eqs. (A3), (A5), and (A6), we have

$$\begin{aligned} \hat{P}_R \Phi_{i\Gamma, n} &= \sum_{n'} \Phi_{i\Gamma, n'} \bar{\Gamma}_{n' n}(\hat{R}) = \sum_{R'} \sum_{n'} \phi_{R'} \bar{S}_{R', i\Gamma n'} \bar{\Gamma}_{n' n}(\hat{R}) \\ &= \hat{P}_R \sum_{R'} \phi_{R'} \bar{S}_{R', i\Gamma n} = \sum_{R'} \phi_{RR'} \bar{S}_{R', i\Gamma n}, \end{aligned} \quad (\text{A7})$$

Then we have

$$\sum_{R'} \sum_{n'} \phi_{R'} \bar{S}_{R', i\Gamma n'} \bar{\Gamma}_{n' n}(\hat{R}) = \sum_{R'} \phi_{RR'} \bar{S}_{R', i\Gamma n}, \quad (\text{A8})$$

$$\bar{S}_{R, i\Gamma n} = \sum_m C_{i\Gamma m} \bar{\Gamma}_{m, n}(R^{-1}), \quad (\text{A9})$$

$$C_{i\Gamma m} = \bar{S}_{i\Gamma m}. \quad (\text{A10})$$

The $C_{i\Gamma m}$ satisfy the orthogonality relations,

$$\frac{l_\Gamma}{G} \delta_{i,i'} = \sum_m C_{i\Gamma m} C_{i'\Gamma m}^*, \quad (\text{A11})$$

$$\frac{l_\Gamma}{G} \delta_{m,m'} = \sum_i C_{i\Gamma m} C_{i\Gamma m'}^*, \quad (\text{A12})$$

where G and l_Γ are the orders of O_h group and irrep Γ , respectively.

5. The inner product of Φ_R and $\Phi_{(i,\Gamma,n)}$

We use the Dirac symbol for the inner product of Φ_R and $\Phi_{(i,\Gamma,n)}$. The normalization is given by

$$\delta_{R,R'} = \langle \Phi_R | \Phi_{R'} \rangle, \quad (\text{A13})$$

$$\delta_{i,i'} \delta_{\Gamma,\Gamma'} \delta_{n,n'} = \langle \Phi_{i,\Gamma,n} | \Phi_{i',\Gamma',n'} \rangle, \quad (\text{A14})$$

If we have some operator, \hat{H} , which is invariant under the rotation, such as the Hamiltonian operator, through Eqs. (A6), (A9), and (A12), we have

$$\begin{aligned} \sum_i \langle \Phi_{i,\Gamma,n} | \hat{H} | \Phi_{i,\Gamma',n'} \rangle &= \sum_i \sum_{R,R'} \bar{S}_{R,i\Gamma n}^* \langle \phi_R | \hat{H} | \phi_{R'} \rangle \bar{S}_{R',i\Gamma' n'} \\ &= \sum_i \sum_{R,R'} \sum_{m,m'} C_{i\Gamma m}^* \bar{\Gamma}_{m,n}^*(R^{-1}) \langle \phi_{R'^{-1}R} | \hat{H} | \phi_I \rangle C_{i\Gamma' m'} \bar{\Gamma}_{m',n'}(R'^{-1}) \\ &= \sum_i \sum_{\tilde{R},R'} \sum_{m,m'} C_{i\Gamma m}^* \bar{\Gamma}_{m,n}^*(\tilde{R}^{-1} R'^{-1}) \langle \phi_{\tilde{R}} | \hat{H} | \phi_I \rangle C_{i\Gamma' m'} \bar{\Gamma}_{m',n'}(\tilde{R}'^{-1}) \\ &= \sum_i \sum_{\tilde{R}} \langle \phi_{\tilde{R}} | \hat{H} | \phi_I \rangle \sum_{m,m'} C_{i\Gamma m}^* C_{i\Gamma' m'} \sum_l \frac{G}{l_\Gamma} \delta_{n,n'} \delta_{\Gamma,\Gamma'} \delta_{l,m'} \bar{\Gamma}_{m,l}^*(\tilde{R}^{-1}) \\ &= \sum_i \sum_{\tilde{R}} \langle \phi_{\tilde{R}} | \hat{H} | \phi_I \rangle \sum_{m,m'} C_{i\Gamma m}^* C_{i\Gamma' m'} \frac{G}{l_\Gamma} \delta_{\Gamma,\Gamma'} \delta_{n,n'} \bar{\Gamma}_{m',m}(\tilde{R}) \\ &= \delta_{\Gamma,\Gamma'} \delta_{n,n'} \sum_{\tilde{R}} \left(\frac{G}{l_\Gamma} \sum_{m,m'} \sum_i C_{i\Gamma m'} \bar{\Gamma}_{m',m}(\tilde{R}) C_{i\Gamma m}^* \right) \langle \phi_{\tilde{R}} | \hat{H} | \phi_I \rangle \\ &= \delta_{\Gamma,\Gamma'} \delta_{n,n'} \sum_{\tilde{R}} \left(\frac{G}{l_\Gamma} \sum_{m,m'} \frac{l_\Gamma}{G} \delta_{m,m'} \bar{\Gamma}_{m',m}(\tilde{R}) \right) \langle \phi_{\tilde{R}} | \hat{H} | \phi_I \rangle \\ &= \delta_{\Gamma,\Gamma'} \delta_{n,n'} \sum_{\tilde{R}} (\chi^\Gamma(\tilde{R})) \langle \phi_{\tilde{R}} | \hat{H} | \phi_I \rangle. \end{aligned} \quad (\text{A15})$$

At last, we find

$$\sum_i \langle \Phi_{i,\Gamma,n} | \hat{H} | \Phi_{i,\Gamma',n'} \rangle = \delta_{\Gamma,\Gamma'} \delta_{n,n'} \sum_R \chi^\Gamma(R) \langle \phi_R | \hat{H} | \phi_I \rangle, \quad (\text{A16})$$

where χ_R^Γ is the character of element \hat{R} in the Γ irrep. The character tables for O_h group and the little group are listed in Table V.

6. The rotation operator in the little group

The O_h group is discussed in detail in the above sections, and it is the symmetry group in the rest frame, i.e., $\mathbf{p} = 0$. In the nonzero momentum system, the symmetry group becomes the subgroup of O_h , named as the little group. In each little group, the rotations satisfying $\hat{R}\mathbf{p} = \mathbf{p}$ will survive. Therefore, for the moving system, one just needs

to keep the surviving rotations and do the same procedure as that in the rest frame. All the rotations for different momentum with $|\mathbf{p}| = 1, 2, 3$ are listed in Table VI.

APPENDIX B: LÜSCHER'S QUANTIZATION CONDITION

The Lüscher formalism provides a model-independent relationship between the phase shifts and the energy levels, assuming exponentially-suppressed finite-volume effects can be safely neglected. In this section we give the relationship between the spectra of irreps considered in this work and the phase shifts up to $\ell = 4$. We have confirmed that the partial waves $\ell = 0$ and $\ell = 2$ agree with previous results reported in Ref. [31]. The general quantization condition equation is summarized by

$$\det[M_{ln,l'n'}^{\Gamma,\mathbf{p}}(q(\Gamma)) - \delta_{l,l'} \delta_{n,n'} \cot \delta_l(q(\Gamma))] = 0, \quad (\text{B1})$$

TABLE VI. The rotation for the each class in the O_h group, C_{4v} , C_{2v} , and C_{3v} for $|\mathbf{p}| = 0, 1, 2$, and 3, respectively.

O_h	\mathbf{p}/Class	I	$8C'_3$	$6C_4$	$6C'_4$	$3C_4^2$	$\hat{\pi}$	$8C'_3 \times \hat{\pi}$	$6C_4 \times \hat{\pi}$	$6C'_4 \times \hat{\pi}$	$3C_4^2 \times \hat{\pi}$
	(0, 0, 0)	\hat{R}_1	\hat{R}_{2-9}	\hat{R}_{10-15}	\hat{R}_{16-21}	\hat{R}_{22-24}	\hat{R}_{25}	\hat{R}_{26-33}	\hat{R}_{33-38}	\hat{R}_{39-44}	\hat{R}_{45-48}
$C_{4\nu}$	\mathbf{p}/Class	I	$2C_4$	$2C'_2 \times \hat{\pi}$	$2C_2 \times \hat{\pi}$	C_2					
	(0, 0, ± 1)	\hat{R}_1	$\hat{R}_{14,15}$	$\hat{R}_{42,43}$	$\hat{R}_{46,47}$	\hat{R}_{24}					
	(0, ± 1 , 0)	\hat{R}_1	$\hat{R}_{12,13}$	$\hat{R}_{44,45}$	$\hat{R}_{46,48}$	\hat{R}_{23}					
	(± 1 , 0, 0)	\hat{R}_1	$\hat{R}_{10,11}$	$\hat{R}_{40,41}$	$\hat{R}_{47,48}$	\hat{R}_{22}					
$C_{2\nu}$	\mathbf{p}/Class	I	C'_2	$C'_2 \times \hat{\pi}$	$C_2 \times \hat{\pi}$						
	(± 1 , ± 1 , 0)	\hat{R}_1	\hat{R}_{18}	\hat{R}_{43}	\hat{R}_{48}						
	(± 1 , 0, ± 1)	\hat{R}_1	\hat{R}_{20}	\hat{R}_{45}	\hat{R}_{47}						
	(0, ± 1 , ± 1)	\hat{R}_1	\hat{R}_{16}	\hat{R}_{41}	\hat{R}_{46}						
	(0, ± 1 , ∓ 1)	\hat{R}_1	\hat{R}_{17}	\hat{R}_{40}	\hat{R}_{46}						
	(± 1 , ∓ 1 , 0)	\hat{R}_1	\hat{R}_{21}	\hat{R}_{44}	\hat{R}_{47}						
	(± 1 , 0, ∓ 1)	\hat{R}_1	\hat{R}_{19}	\hat{R}_{42}	\hat{R}_{48}						
$C_{3\nu}$	\mathbf{p}/Class	I	$2C_3$	$3C'_2 \times \hat{\pi}$							
	(± 1 , ± 1 , ± 1)	\hat{R}_1	$\hat{R}_{2,3}$	$\hat{R}_{41,43,45}$							
	(± 1 , ± 1 , ∓ 1)	\hat{R}_1	$\hat{R}_{6,7}$	$\hat{R}_{40,43,44}$							
	(± 1 , ∓ 1 , ± 1)	\hat{R}_1	$\hat{R}_{8,9}$	$\hat{R}_{40,42,45}$							
	(∓ 1 , ± 1 , ± 1)	\hat{R}_1	$\hat{R}_{4,5}$	$\hat{R}_{41,42,44}$							

where Γ , \mathbf{p} , $l(l')$, and $n(n')$ indicate the irrep, total momentum, angular momentum, and the n th Γ appearing in the representation of this angular momentum, respectively. $q(\Gamma)$ is the on-shell momentum of the energy level of irrep Γ in the center of mass (c.m.) system.

The matrix M is calculated from

$$M_{ln,l'n'}^{\Gamma,\mathbf{p}}(q(\Gamma)) = \sum_{m,m'} C_{l,m}^{\Gamma,\alpha,n*} C_{l',m'}^{\Gamma,\alpha,n'} M_{lm,l'm'}^{\mathbf{p}}(q(\Gamma)), \quad (\text{B2})$$

$$M_{lm,l'm'}^{\mathbf{p}}(q(\Gamma)) = (-1)^l \sum_{j=|l-l'|}^{l+l'} \sum_{s=-j}^j i^j \sqrt{2j+1} \omega_{js}^{\mathbf{d}=\mathbf{p}L/2\pi} \times (\tilde{q} = q(\Gamma)L/2\pi) C_{lm,js,l'm'}, \quad (\text{B3})$$

$$\omega_{js}^{\mathbf{d}}(\tilde{q}) = \frac{1}{\pi^{3/2} \sqrt{2j+1}} \frac{Z_{js}^{\mathbf{d}}(1, \tilde{q})^{-1}}{\gamma \tilde{q}^{j+1}}, \quad (\text{B4})$$

where α runs from 1 to the dimension of Γ . γ is the Lorentz factor

$$\gamma = \frac{W}{E_{\text{C.M.}}} = \frac{\sqrt{\mathbf{p}^2 + E_{\text{C.M.}}^2}}{E_{\text{C.M.}}}, \quad (\text{B5})$$

where $E_{\text{C.M.}} = 2\sqrt{q^2 + m_\pi^2}$ is the energy level in the c.m. system.

The factor $C_{lm,js,l'm'}$ is related to the Wigner 3- j symbols as follows:

$$C_{lm,js,l'm'} = (-1)^{m'} i^{l-j+l'} \sqrt{(2l+1)(2j+1)(2l'+1)} \times \begin{pmatrix} l & j & l' \\ m & s & -m' \end{pmatrix} \begin{pmatrix} l & j & l' \\ 0 & 0 & 0 \end{pmatrix}. \quad (\text{B6})$$

Now we only need to know the coefficients $C_{l,m}^{\Gamma,\alpha,n}$ in Eq. (B2). We give these values in Table VII for the moving system, while for the rest frame, the matrices $M_{ln,l'n'}^{\Gamma,\mathbf{p}}(q(\Gamma))$ can be read from Ref. [26]. It is worth mentioning that in our calculation we average over all momenta with fixed $|\mathbf{p}|$. Since the spectra of them are the same, we choose one case to list each $C_{l,m}^{\Gamma,\alpha,n}$. Finally, Eq. (B1) for each case are listed in the following.

For the A_1 irrep in the rest frame, $\mathbf{d} = \mathbf{p}L/2\pi = \mathbf{0}$,

$$0 = \det \begin{pmatrix} -\cot \delta_0 + \omega_{00}^{\mathbf{d}} & \frac{6\sqrt{21}}{7} \omega_{40}^{\mathbf{d}} \\ \frac{6\sqrt{21}}{7} \omega_{40}^{\mathbf{d}} & -\cot \delta_4 + \omega_{00}^{\mathbf{d}} + \frac{324}{143} \omega_{40}^{\mathbf{d}} + \frac{80}{11} \omega_{60}^{\mathbf{d}} + \frac{560}{143} \omega_{80}^{\mathbf{d}} \end{pmatrix}. \quad (\text{B7})$$

For the E irrep in the rest frame, $\mathbf{d} = \mathbf{0}$,

TABLE VII. The relationship between angular momentum and irrep at momenta up to $P^2 = 3P_0^2$.

\mathbf{p}	l	n	Γ	α	$C_{l,m}^{\Gamma,\alpha,n} l, m\rangle$
(0, 0, 1)	0	1	A_1	1	$ 0, 0\rangle$
		2	A_1	1	$ 2, 0\rangle$
	1	1	B_1	1	$\frac{1}{\sqrt{2}}(2, -2\rangle + 2, 2\rangle)$
		1	B_2	1	$\frac{1}{\sqrt{2}}(2, -2\rangle - 2, 2\rangle)$
		1	E	1	$\frac{1}{\sqrt{2}}(2, -1\rangle - i 2, 1\rangle)$
				2	$\frac{1-i}{2}(2, -1\rangle + i 2, 1\rangle)$
	4	1	A_1	1	$\frac{1}{2}(4, -4\rangle + \sqrt{2} 4, 0\rangle + 4, 4\rangle)$
		2	A_1	1	$\frac{1}{2}(4, -4\rangle - \sqrt{2} 4, 0\rangle + 4, 4\rangle)$
		1	A_2	1	$\frac{1}{\sqrt{2}}(- 4, -4\rangle + 4, 4\rangle)$
		1	B_1	1	$\frac{1}{\sqrt{2}}(4, -2\rangle + 4, 2\rangle)$
		1	B_2	1	$\frac{1}{\sqrt{2}}(- 4, -2\rangle + 4, 2\rangle)$
		1	E	1	$\frac{1+i}{2\sqrt{2}}(- 4, -3\rangle + 4, -1\rangle - i 4, 1\rangle - i 4, 3\rangle)$
				2	$\frac{1}{2}(4, -3\rangle + 4, -1\rangle + i 4, 1\rangle - i 4, 3\rangle)$
		2	E	1	$\frac{1+i}{2\sqrt{2}}(4, -3\rangle + 4, -1\rangle - i 4, 1\rangle + i 4, 3\rangle)$
				2	$\frac{1}{2}(- 4, -3\rangle + 4, -1\rangle + i 4, 1\rangle + i 4, 3\rangle)$
(1, 1, 0)	0	1	A_1	1	$ 0, 0\rangle$
	2	1	A_1	1	$ 2, 0\rangle$
		2	A_1	1	$\frac{1}{\sqrt{2}}(2, -2\rangle - 2, 2\rangle)$
		1	A_2	1	$\frac{1}{\sqrt{2}}(2, -1\rangle - i 2, 1\rangle)$
	4	1	B_1	1	$\frac{1}{\sqrt{2}}(2, -1\rangle + i 2, 1\rangle)$
		1	B_2	1	$\frac{1}{\sqrt{2}}(2, -2\rangle + 2, 2\rangle)$
		1	A_1	1	$\frac{1}{2}(4, -4\rangle - 4, -2\rangle + 4, 2\rangle + 4, 4\rangle)$
		2	A_1	1	$\frac{1}{2}(4, -4\rangle + 4, -2\rangle - 4, 2\rangle + 4, 4\rangle)$
		3	A_1	1	$ 4, 0\rangle$
		1	A_2	1	$\frac{1}{2}(4, -3\rangle + 4, -1\rangle - i 4, 1\rangle + i 4, 3\rangle)$
		2	A_2	1	$\frac{1}{2}(4, -3\rangle - 4, -1\rangle + i 4, 1\rangle + i 4, 3\rangle)$
		1	B_1	1	$\frac{1}{2}(4, -3\rangle + 4, -1\rangle + i 4, 1\rangle - i 4, 3\rangle)$
		2	B_1	1	$\frac{1}{2}(4, -3\rangle - 4, -1\rangle - i 4, 1\rangle - i 4, 3\rangle)$
	2	1	B_2	1	$\frac{1}{2}(- 4, -4\rangle + 4, -2\rangle + 4, 2\rangle + 4, 4\rangle)$
		2	B_2	1	$\frac{1}{2}(4, -4\rangle + 4, -2\rangle + 4, 2\rangle - 4, 4\rangle)$
(1, 1, 1)	0	1	A_1	1	$ 0, 0\rangle$
	2	1	A_1	1	$\frac{1}{\sqrt{6}}(2, -2\rangle + (1-i) 2, -1\rangle + (1+i) 2, 1\rangle - 2, 2\rangle)$
		1	E	1	$\frac{1}{\sqrt{2}}(2, -2\rangle + 2, 2\rangle)$
				2	$- 2, 0\rangle$
		2	E	1	$\frac{1}{\sqrt{2}}(2, -1\rangle - i 2, 1\rangle)$
				2	$\frac{1}{\sqrt{6}}(-(1-i) 2, -2\rangle - i 2, -1\rangle + 2, 1\rangle + (1-i) 2, 2\rangle)$
	4	1	A_1	1	$\frac{1}{2}\sqrt{\frac{5}{6}}(4, -4\rangle + \sqrt{\frac{14}{5}} 4, 0\rangle + 4, 4\rangle)$
		2	A_1	1	$\frac{1}{2}\left(-\sqrt{\frac{7}{6}} 4, -3\rangle + \frac{-1+i}{\sqrt{3}} 4, -2\rangle + \frac{-i}{\sqrt{6}} 4, -1\rangle + \frac{1}{\sqrt{6}} 4, 1\rangle + \frac{1-i}{\sqrt{3}} 4, 2\rangle + i\sqrt{\frac{7}{6}} 4, 3\rangle\right)$
		3	A_2	1	$\frac{1}{2}\left(\frac{-1+i}{\sqrt{3}} 4, -4\rangle - \frac{i}{\sqrt{6}} 4, -3\rangle + \sqrt{\frac{2}{6}} 4, -1\rangle - i\sqrt{\frac{2}{6}} 4, 1\rangle + \frac{1}{\sqrt{6}} 4, 3\rangle + \frac{1-i}{\sqrt{3}} 4, 4\rangle\right)$
		1	E	1	$\frac{1}{4}(-i\sqrt{7} 4, -3\rangle - 4, -1\rangle + i 4, 1\rangle + \sqrt{7} 4, 3\rangle)$
		E	2	$\frac{1}{4}\left(\sqrt{\frac{7}{3}} 4, -3\rangle + \frac{4(-1+i)}{\sqrt{6}} 4, -2\rangle + \frac{i}{\sqrt{3}} 4, -1\rangle - \frac{1}{\sqrt{3}} 4, 1\rangle + \frac{4(1-i)}{\sqrt{6}} 4, 2\rangle - i\sqrt{\frac{7}{3}} 4, 4\rangle\right)$	
				$-\frac{1}{\sqrt{2}}(4, -2\rangle + 4, 2\rangle)$	
		2	E	1	$\frac{1}{2}\left(\sqrt{\frac{2}{6}} 4, -4\rangle - \sqrt{\frac{5}{3}} 4, 0\rangle + \sqrt{\frac{2}{6}} 4, 4\rangle\right)$
		3	E	1	$\frac{1}{\sqrt{3}}(- 4, -4\rangle - \frac{1-i}{4\sqrt{2}} 4, -3\rangle - \frac{\sqrt{7}(1+i)}{4\sqrt{2}} 4, -1\rangle + \frac{\sqrt{7}(-1+i)}{4\sqrt{2}} 4, 1\rangle - \frac{1+i}{4\sqrt{2}} 4, 3\rangle + 4, 4\rangle)$
				2	$\frac{1+i}{4\sqrt{2}}(4, -3\rangle - i\sqrt{7} 4, -1\rangle + \sqrt{7} 4, 1\rangle - i 4, 3\rangle)$

$$0 = \det \begin{pmatrix} -\cot \delta_2 + \omega_{00}^{\mathbf{d}} + \frac{18}{7} \omega_{40}^{\mathbf{d}} & -\frac{120\sqrt{3}}{77} \omega_{40}^{\mathbf{d}} - \frac{30\sqrt{3}}{11} \omega_{60}^{\mathbf{d}} \\ -\frac{120\sqrt{3}}{77} \omega_{40}^{\mathbf{d}} - \frac{30\sqrt{3}}{11} \omega_{60}^{\mathbf{d}} & -\cot \delta_4 + \omega_{00}^{\mathbf{d}} + \frac{324}{1001} \omega_{40}^{\mathbf{d}} - \frac{64}{11} \omega_{60}^{\mathbf{d}} + \frac{392}{143} \omega_{80}^{\mathbf{d}} \end{pmatrix}. \quad (\text{B8})$$

For the T_2 irrep in the rest frame, $\mathbf{d} = \mathbf{0}$,

$$0 = \det \begin{pmatrix} -\cot \delta_2 + \omega_{00}^{\mathbf{d}} - \frac{12}{7} \omega_{40}^{\mathbf{d}} & -\frac{60\sqrt{3}}{77} \omega_{40}^{\mathbf{d}} - \frac{40\sqrt{3}}{11} \omega_{60}^{\mathbf{d}} \\ -\frac{60\sqrt{3}}{77} \omega_{40}^{\mathbf{d}} - \frac{40\sqrt{3}}{11} \omega_{60}^{\mathbf{d}} & -\cot \delta_4 + \omega_{00}^{\mathbf{d}} - \frac{162}{77} \omega_{40}^{\mathbf{d}} + \frac{20}{11} \omega_{60}^{\mathbf{d}} \end{pmatrix}. \quad (\text{B9})$$

For the A_1 irrep in the moving frame with $|\mathbf{p}L/2\pi| = 1$, we choose $\mathbf{d} = \mathbf{p}L/2\pi = (0, 0, 1)$,

$$0 = \det \begin{pmatrix} -\cot \delta_0 + \omega_{00}^{\mathbf{d}} & -\sqrt{5} \omega_{20}^{\mathbf{d}} & \frac{3}{\sqrt{2}} \omega_{40}^{\mathbf{d}} + 3 \omega_{44}^{\mathbf{d}} & -\frac{3}{\sqrt{2}} \omega_{40}^{\mathbf{d}} + 3 \omega_{44}^{\mathbf{d}} \\ -\sqrt{5} \omega_{20}^{\mathbf{d}} & -\cot \delta_2 + M_{21,21}^{A_1, \mathbf{p}} & M_{21,41}^{A_1, \mathbf{p}} & M_{21,42}^{A_1, \mathbf{p}} \\ \frac{3}{\sqrt{2}} \omega_{40}^{\mathbf{d}} + 3 \omega_{44}^{\mathbf{d}} & M_{21,41}^{A_1, \mathbf{p}} & -\cot \delta_4 + M_{41,41}^{A_1, \mathbf{p}} & M_{41,42}^{A_1, \mathbf{p}} \\ -\frac{3}{\sqrt{2}} \omega_{40}^{\mathbf{d}} + 3 \omega_{44}^{\mathbf{d}} & M_{21,41}^{A_1, \mathbf{p}} & M_{41,42}^{A_1, \mathbf{p}} & -\cot \delta_4 + M_{42,42}^{A_1, \mathbf{p}} \end{pmatrix}, \quad (\text{B10})$$

where

$$\begin{aligned} M_{21,21}^{A_1, \mathbf{p}} &= \omega_{00}^{\mathbf{d}} + \frac{10}{7} \omega_{20}^{\mathbf{d}} + \frac{18}{7} \omega_{40}^{\mathbf{d}}, \\ M_{21,41}^{A_1, \mathbf{p}} &= -\frac{3\sqrt{10}}{7} \omega_{20}^{\mathbf{d}} + \frac{12\sqrt{5}}{11} \omega_{44}^{\mathbf{d}} - \frac{15}{11} \omega_{64}^{\mathbf{d}} - \frac{30\sqrt{10}}{77} \omega_{40}^{\mathbf{d}} - \frac{15\sqrt{10}}{22} \omega_{60}^{\mathbf{d}}, \\ M_{21,42}^{A_1, \mathbf{p}} &= +\frac{3\sqrt{10}}{7} \omega_{20}^{\mathbf{d}} + \frac{12\sqrt{5}}{11} \omega_{44}^{\mathbf{d}} - \frac{15}{11} \omega_{64}^{\mathbf{d}} + \frac{30\sqrt{10}}{77} \omega_{40}^{\mathbf{d}} + \frac{15\sqrt{10}}{22} \omega_{60}^{\mathbf{d}}, \\ M_{41,41}^{A_1, \mathbf{p}} &= +\omega_{00}^{\mathbf{d}} - \frac{20}{77} \omega_{20}^{\mathbf{d}} + \frac{1296}{1001} \omega_{40}^{\mathbf{d}} + \frac{8}{11} \omega_{60}^{\mathbf{d}} + \frac{497}{286} \omega_{80}^{\mathbf{d}} + \frac{162\sqrt{2}}{143} \omega_{44}^{\mathbf{d}} - \frac{12\sqrt{10}}{11} \omega_{64}^{\mathbf{d}} + \frac{42}{13} \sqrt{\frac{5}{22}} \omega_{84}^{\mathbf{d}} + 21 \sqrt{\frac{5}{286}} \omega_{88}^{\mathbf{d}}, \\ M_{41,42}^{A_1, \mathbf{p}} &= -\frac{120}{77} \omega_{20}^{\mathbf{d}} - \frac{162}{1001} \omega_{40}^{\mathbf{d}} - \frac{12}{11} \omega_{60}^{\mathbf{d}} - \frac{483}{286} \omega_{80}^{\mathbf{d}} + 21 \sqrt{\frac{5}{286}} \omega_{88}^{\mathbf{d}}, \\ M_{42,42}^{A_1, \mathbf{p}} &= +\omega_{00}^{\mathbf{d}} - \frac{20}{77} \omega_{20}^{\mathbf{d}} + \frac{1296}{1001} \omega_{40}^{\mathbf{d}} + \frac{8}{11} \omega_{60}^{\mathbf{d}} + \frac{497}{286} \omega_{80}^{\mathbf{d}} - \frac{162\sqrt{2}}{143} \omega_{44}^{\mathbf{d}} + \frac{12\sqrt{10}}{11} \omega_{64}^{\mathbf{d}} - \frac{42}{13} \sqrt{\frac{5}{22}} \omega_{84}^{\mathbf{d}} + 21 \sqrt{\frac{5}{286}} \omega_{88}^{\mathbf{d}}. \end{aligned}$$

For the B_1 irrep in the moving frame with $|\mathbf{p}L/2\pi| = 1$, we choose $\mathbf{d} = \mathbf{p}L/2\pi = (0, 0, 1)$,

$$0 = \det \begin{pmatrix} -\cot \delta_2 + \omega_{00}^{\mathbf{d}} - \frac{10}{7} \omega_{20}^{\mathbf{d}} + \frac{3}{7} \omega_{40}^{\mathbf{d}} + 6\sqrt{\frac{5}{14}} \omega_{44}^{\mathbf{d}} & M_{21,41}^{B_1, \mathbf{p}} \\ M_{21,41}^{B_1, \mathbf{p}} & -\cot \delta_4 + M_{41,41}^{B_1, \mathbf{p}} \end{pmatrix}, \quad (\text{B11})$$

where

$$\begin{aligned} M_{21,41}^{B_1, \mathbf{p}} &= -\frac{5\sqrt{3}}{7} \omega_{20}^{\mathbf{d}} + \frac{90\sqrt{3}}{77} \omega_{40}^{\mathbf{d}} - \frac{5\sqrt{3}}{11} \omega_{60}^{\mathbf{d}} + \frac{6\sqrt{210}}{77} \omega_{44}^{\mathbf{d}} - \frac{5\sqrt{42}}{11} \omega_{64}^{\mathbf{d}}, \\ M_{41,41}^{B_1, \mathbf{p}} &= +\omega_{00}^{\mathbf{d}} + \frac{40}{77} \omega_{20}^{\mathbf{d}} - \frac{81}{91} \omega_{40}^{\mathbf{d}} - 2\omega_{60}^{\mathbf{d}} + \frac{196}{143} \omega_{80}^{\mathbf{d}} + \frac{243}{143} \sqrt{\frac{10}{7}} \omega_{44}^{\mathbf{d}} + \frac{6\sqrt{14}}{11} \omega_{64}^{\mathbf{d}} + \frac{42}{13} \sqrt{\frac{14}{11}} \omega_{84}^{\mathbf{d}}. \end{aligned}$$

For the B_2 irrep in the moving frame with $|\mathbf{p}L/2\pi| = 1$, we choose $\mathbf{d} = \mathbf{p}L/2\pi = (0, 0, 1)$,

$$0 = \det \begin{pmatrix} -\cot \delta_2 + \omega_{00}^{\mathbf{d}} - \frac{10}{7}\omega_{00}^{\mathbf{d}} + \frac{3}{7}\omega_{40}^{\mathbf{d}} - \frac{3\sqrt{70}}{7}\omega_{44}^{\mathbf{d}} & M_{21,41}^{B_2, \mathbf{p}} \\ M_{21,41}^{B_2, \mathbf{p}} & -\cot \delta_4 + M_{41,41}^{B_2, \mathbf{p}} \end{pmatrix}, \quad (\text{B12})$$

where

$$M_{21,41}^{B_2, \mathbf{p}} = +\frac{5\sqrt{3}}{7}\omega_{20}^{\mathbf{d}} - \frac{90\sqrt{3}}{77}\omega_{40}^{\mathbf{d}} + \frac{5\sqrt{3}}{11}\omega_{60}^{\mathbf{d}} + \frac{6\sqrt{210}}{77}\omega_{44}^{\mathbf{d}} - \frac{5\sqrt{42}}{11}\omega_{64}^{\mathbf{d}},$$

$$M_{41,41}^{B_2, \mathbf{p}} = +\omega_{00}^{\mathbf{d}} + \frac{40}{77}\omega_{20}^{\mathbf{d}} - \frac{81}{91}\omega_{40}^{\mathbf{d}} - 2\omega_{60}^{\mathbf{d}} + \frac{196}{143}\omega_{80}^{\mathbf{d}} - \frac{243}{143}\sqrt{\frac{10}{7}}\omega_{44}^{\mathbf{d}} - \frac{6\sqrt{14}}{11}\omega_{64}^{\mathbf{d}} - \frac{42}{13}\sqrt{\frac{14}{11}}\omega_{84}^{\mathbf{d}}.$$

For the E irrep in the moving frame with $|\mathbf{p}L/2\pi| = 1$, we choose $\mathbf{d} = \mathbf{p}L/2\pi = (0, 0, 1)$,

$$0 = \det \begin{pmatrix} -\cot \delta_2 + \omega_{00}^{\mathbf{d}} + \frac{5}{7}\omega_{20}^{\mathbf{d}} - \frac{12}{7}\omega_{40}^{\mathbf{d}} & M_{21,41}^{E, \mathbf{p}} & M_{21,41}^{E, \mathbf{p}} \\ M_{21,41}^{E, \mathbf{p}} & -\cot \delta_4 + M_{41,41}^{E, \mathbf{p}} & M_{41,42}^{E, \mathbf{p}} \\ M_{21,41}^{E, \mathbf{p}} & M_{41,42}^{E, \mathbf{p}} & -\cot \delta_4 + M_{41,41}^{E, \mathbf{p}} \end{pmatrix}, \quad (\text{B13})$$

where

$$M_{21,41}^{E, \mathbf{p}} = -\frac{5\sqrt{3}}{7}\omega_{20}^{\mathbf{d}} - \frac{15\sqrt{3}}{77}\omega_{40}^{\mathbf{d}} + \frac{10\sqrt{3}}{11}\omega_{60}^{\mathbf{d}} - i\frac{3\sqrt{30}}{11}\omega_{44}^{\mathbf{d}} - i\frac{10\sqrt{6}}{11}\omega_{64}^{\mathbf{d}},$$

$$M_{41,41}^{E, \mathbf{p}} = +\omega_{00}^{\mathbf{d}} + \frac{25}{77}\omega_{20}^{\mathbf{d}} - \frac{486}{1001}\omega_{40}^{\mathbf{d}} + \frac{8}{11}\omega_{60}^{\mathbf{d}} - \frac{224}{143}\omega_{80}^{\mathbf{d}},$$

$$M_{41,42}^{E, \mathbf{p}} = +\frac{60}{77}\omega_{20}^{\mathbf{d}} + \frac{1215}{1001}\omega_{40}^{\mathbf{d}} - \frac{9}{11}\omega_{60}^{\mathbf{d}} - \frac{168}{143}\omega_{80}^{\mathbf{d}} + i\frac{81\sqrt{10}}{143}\omega_{44}^{\mathbf{d}} + i\frac{3\sqrt{2}}{11}\omega_{64}^{\mathbf{d}} - i\frac{84}{13}\sqrt{\frac{2}{11}}\omega_{84}^{\mathbf{d}}.$$

For the A_1 irrep in the moving frame with $|\mathbf{p}L/2\pi| = \sqrt{2}$, we choose $\mathbf{d} = \mathbf{p}L/2\pi = (1, 1, 0)$,

$$0 = \det \begin{pmatrix} -\cot \delta_0 + \omega_{00}^{\mathbf{d}} & -\sqrt{5}\omega_{20}^{\mathbf{d}} & \sqrt{10}\omega_{22}^{\mathbf{d}} & 3(\omega_{44}^{\mathbf{d}} + \omega_{42}^{\mathbf{d}}) & 3(\omega_{44}^{\mathbf{d}} - \omega_{42}^{\mathbf{d}}) & 3\omega_{40}^{\mathbf{d}} \\ -\sqrt{5}\omega_{20}^{\mathbf{d}} & -\cot \delta_2 + M_{21,21}^{A_1, \mathbf{p}} & M_{21,22}^{A_1, \mathbf{p}} & M_{21,41}^{A_1, \mathbf{p}} & M_{21,41}^{A_1, \mathbf{p}} & M_{21,43}^{A_1, \mathbf{p}} \\ -\sqrt{10}\omega_{22}^{\mathbf{d}} & M_{21,22}^{A_1, \mathbf{p}} & M_{22,22}^{A_1, \mathbf{p}} - \cot \delta_2 & M_{22,41}^{A_1, \mathbf{p}} & -M_{22,41}^{A_1, \mathbf{p}} & M_{22,43}^{A_1, \mathbf{p}} \\ 3(\omega_{44}^{\mathbf{d}} - \omega_{42}^{\mathbf{d}}) & M_{21,41}^{A_1, \mathbf{p}} & M_{22,41}^{A_1, \mathbf{p}} & M_{41,41}^{A_1, \mathbf{p}} - \cot \delta_4 & M_{41,42}^{A_1, \mathbf{p}} & M_{41,43}^{A_1, \mathbf{p}} \\ 3(\omega_{44}^{\mathbf{d}} + \omega_{42}^{\mathbf{d}}) & M_{21,41}^{A_1, \mathbf{p}} & -M_{22,41}^{A_1, \mathbf{p}} & M_{41,42}^{A_1, \mathbf{p}} & M_{41,41}^{A_1, \mathbf{p}} - \cot \delta_4 & M_{41,43}^{A_1, \mathbf{p}} \\ 3\omega_{40}^{\mathbf{d}} & M_{21,43}^{A_1, \mathbf{p}} & M_{22,43}^{A_1, \mathbf{p}} & M_{41,43}^{A_1, \mathbf{p}} & M_{41,43}^{A_1, \mathbf{p}} & M_{43,43}^{A_1, \mathbf{p}} - \cot \delta_4 \end{pmatrix}, \quad (\text{B14})$$

where

$$M_{21,21}^{A_1, \mathbf{p}} = \omega_{00}^{\mathbf{d}} + \frac{10}{7}\omega_{20}^{\mathbf{d}} + \frac{18}{7}\omega_{40}^{\mathbf{d}},$$

$$M_{21,22}^{A_1, \mathbf{p}} = \frac{10\sqrt{2}}{7}\omega_{22}^{\mathbf{d}} - \frac{3\sqrt{30}}{7}\omega_{42}^{\mathbf{d}},$$

$$M_{21,41}^{A_1, \mathbf{p}} = -\frac{5\sqrt{10}}{7}\omega_{22}^{\mathbf{d}} - \frac{24\sqrt{5}}{77}\omega_{42}^{\mathbf{d}} - \frac{2\sqrt{210}}{11}\omega_{62}^{\mathbf{d}} + \frac{12\sqrt{5}}{11}\omega_{44}^{\mathbf{d}} - \frac{15}{11}\omega_{64}^{\mathbf{d}},$$

$$M_{21,43}^{A_1, \mathbf{p}} = -\frac{6\sqrt{5}}{77}\omega_{20}^{\mathbf{d}} - \frac{60\sqrt{5}}{77}\omega_{40}^{\mathbf{d}} - \frac{15}{11}\omega_{60}^{\mathbf{d}},$$

$$M_{22,22}^{A_1, \mathbf{p}} = \omega_{00}^{\mathbf{d}} - \frac{10}{7}\omega_{20}^{\mathbf{d}} + \frac{3}{7}\omega_{40}^{\mathbf{d}} - 6\sqrt{\frac{5}{14}}\omega_{44}^{\mathbf{d}},$$

$$\begin{aligned}
M_{22,41}^{A_1, \mathbf{p}} &= +\frac{5\sqrt{6}}{14}\omega_{20}^{\mathbf{d}} - \frac{45\sqrt{6}}{77}\omega_{40}^{\mathbf{d}} + \frac{5\sqrt{6}}{22}\omega_{60}^{\mathbf{d}} + \frac{5\sqrt{7}}{7}\omega_{22}^{\mathbf{d}} - \frac{6\sqrt{105}}{77}\omega_{42}^{\mathbf{d}} + \frac{\sqrt{10}}{22}\omega_{62}^{\mathbf{d}} + \frac{6\sqrt{105}}{77}\omega_{44}^{\mathbf{d}} - \frac{5\sqrt{21}}{11}\omega_{64}^{\mathbf{d}} - \frac{15}{\sqrt{22}}\omega_{66}^{\mathbf{d}}, \\
M_{22,43}^{A_1, \mathbf{p}} &= -\frac{\sqrt{10}}{7}\omega_{22}^{\mathbf{d}} + \frac{90\sqrt{6}}{77}\omega_{42}^{\mathbf{d}} - \frac{10\sqrt{7}}{11}\omega_{62}^{\mathbf{d}}, \\
M_{41,41}^{A_1, \mathbf{p}} &= \omega_{00}^{\mathbf{d}} - \frac{50}{77}\omega_{20}^{\mathbf{d}} + \frac{243}{2002}\omega_{40}^{\mathbf{d}} - \frac{13}{11}\omega_{60}^{\mathbf{d}} + \frac{203}{286}\omega_{80}^{\mathbf{d}} - \frac{243}{143}\sqrt{\frac{5}{14}}\omega_{44}^{\mathbf{d}} - \frac{3\sqrt{14}}{11}\omega_{64}^{\mathbf{d}} - \frac{42}{13}\sqrt{\frac{7}{22}}\omega_{84}^{\mathbf{d}} + 21\sqrt{\frac{5}{286}}\omega_{88}^{\mathbf{d}}, \\
M_{41,42}^{A_1, \mathbf{p}} &= -\frac{90}{77}\omega_{20}^{\mathbf{d}} + \frac{2025}{2002}\omega_{40}^{\mathbf{d}} + \frac{9}{11}\omega_{60}^{\mathbf{d}} - \frac{189}{286}\omega_{80}^{\mathbf{d}} - \frac{10}{11}\sqrt{\frac{6}{7}}\omega_{22}^{\mathbf{d}} + \frac{243}{143}\sqrt{\frac{10}{7}}\omega_{42}^{\mathbf{d}} - \frac{4\sqrt{15}}{11}\omega_{62}^{\mathbf{d}} + \frac{21\sqrt{5}}{143}\omega_{82}^{\mathbf{d}} + \frac{243}{143}\sqrt{\frac{5}{14}}\omega_{44}^{\mathbf{d}} \\
&\quad + \frac{3\sqrt{14}}{11}\omega_{64}^{\mathbf{d}} + \frac{42}{13}\sqrt{\frac{7}{22}}\omega_{84}^{\mathbf{d}} + 4\sqrt{\frac{3}{11}}\omega_{66}^{\mathbf{d}} - 7\sqrt{\frac{21}{143}}\omega_{86}^{\mathbf{d}} + 21\sqrt{\frac{5}{286}}\omega_{88}^{\mathbf{d}}, \\
M_{41,43}^{A_1, \mathbf{p}} &= +\frac{30\sqrt{15}}{77}\omega_{22}^{\mathbf{d}} + \frac{81}{91}\omega_{42}^{\mathbf{d}} - \frac{105\sqrt{14}}{143}\omega_{82}^{\mathbf{d}} + \frac{162}{143}\omega_{44}^{\mathbf{d}} - \frac{12\sqrt{5}}{11}\omega_{64}^{\mathbf{d}} + \frac{21}{13}\sqrt{\frac{5}{11}}\omega_{84}^{\mathbf{d}}, \\
M_{43,43}^{A_1, \mathbf{p}} &= \omega_{00}^{\mathbf{d}} + \frac{100}{77}\omega_{20}^{\mathbf{d}} + \frac{1458}{1001}\omega_{40}^{\mathbf{d}} + \frac{20}{11}\omega_{60}^{\mathbf{d}} + \frac{490}{143}\omega_{80}^{\mathbf{d}}.
\end{aligned}$$

For the A_2 irrep in moving frame with $|\mathbf{p}L/2\pi| = \sqrt{2}$, we choose $\mathbf{d} = \mathbf{p}L/2\pi = (1, 1, 0)$,

$$0 = \det \begin{pmatrix} -\cot \delta_0 + M_{21,21}^{A_2, \mathbf{p}} & M_{21,41}^{A_2, \mathbf{p}} & -M_{21,41}^{A_2, \mathbf{p}} \\ M_{21,41}^{A_2, \mathbf{p}} & -\cot \delta_4 + M_{41,41}^{A_2, \mathbf{p}} & M_{41,42}^{A_2, \mathbf{p}} \\ -M_{21,41}^{A_2, \mathbf{p}} & M_{41,42}^{A_2, \mathbf{p}} & -\cot \delta_4 + M_{41,41}^{A_2, \mathbf{p}} \end{pmatrix}, \quad (\text{B15})$$

where

$$\begin{aligned}
M_{21,21}^{A_2, \mathbf{p}} &= \omega_{00}^{\mathbf{d}} + \frac{5}{7}\omega_{20}^{\mathbf{d}} - \frac{12}{7}\omega_{40}^{\mathbf{d}} + i\frac{\sqrt{30}}{7}(\sqrt{5}\omega_{22}^{\mathbf{d}} + 2\sqrt{3}\omega_{42}^{\mathbf{d}}), \\
M_{21,41}^{A_2, \mathbf{p}} &= -\frac{5\sqrt{3}}{7}\omega_{20}^{\mathbf{d}} - \frac{15\sqrt{3}}{77}\omega_{40}^{\mathbf{d}} + \frac{10\sqrt{3}}{11}\omega_{60}^{\mathbf{d}} + \frac{5\sqrt{2}}{14}(i + \sqrt{7})\omega_{22}^{\mathbf{d}} + \frac{3}{11}\sqrt{\frac{15}{14}}\left(5 - i\frac{9}{\sqrt{7}}\right)\omega_{42}^{\mathbf{d}} - \frac{4\sqrt{5}}{11}(1 + i\sqrt{7})\omega_{62}^{\mathbf{d}} \\
&\quad + i\frac{3\sqrt{30}}{11}\omega_{44}^{\mathbf{d}} + i\frac{10\sqrt{6}}{11}\omega_{64}^{\mathbf{d}}, \\
M_{41,41}^{A_2, \mathbf{p}} &= +\omega_{00}^{\mathbf{d}} + \frac{25}{77}\omega_{20}^{\mathbf{d}} - \frac{486}{1001}\omega_{40}^{\mathbf{d}} + \frac{8}{11}\omega_{60}^{\mathbf{d}} - \frac{224}{143}\omega_{80}^{\mathbf{d}} + i\frac{25\sqrt{6}}{77}\omega_{22}^{\mathbf{d}} + i\frac{243\sqrt{10}}{1001}\omega_{42}^{\mathbf{d}} + i\frac{\sqrt{105}}{11}\omega_{62}^{\mathbf{d}} \\
&\quad + i\frac{42\sqrt{35}}{143}\omega_{82}^{\mathbf{d}} - i\sqrt{\frac{21}{11}}\omega_{66}^{\mathbf{d}} - i14\sqrt{\frac{3}{143}}\omega_{86}^{\mathbf{d}}, \\
M_{41,42}^{A_2, \mathbf{p}} &= -\frac{60}{77}\omega_{20}^{\mathbf{d}} - \frac{1215}{1001}\omega_{40}^{\mathbf{d}} + \frac{9}{11}\omega_{60}^{\mathbf{d}} + \frac{168}{143}\omega_{80}^{\mathbf{d}} + \frac{5\sqrt{6}}{77}(3\sqrt{7} - i5)\omega_{22}^{\mathbf{d}} + \frac{81\sqrt{10}}{1001}(-\sqrt{7} - i3)\omega_{42}^{\mathbf{d}} + \frac{\sqrt{15}}{11}(-6 - i\sqrt{7})\omega_{62}^{\mathbf{d}} \\
&\quad + \frac{42\sqrt{5}}{143}(2 - i\sqrt{7})\omega_{82}^{\mathbf{d}} + i\frac{81\sqrt{10}}{143}\omega_{44}^{\mathbf{d}} + i\frac{3\sqrt{2}}{11}\omega_{64}^{\mathbf{d}} - i\frac{84}{13}\sqrt{\frac{2}{11}}\omega_{84}^{\mathbf{d}} - i\sqrt{\frac{21}{11}}\omega_{66}^{\mathbf{d}} - i14\sqrt{\frac{3}{143}}\omega_{86}^{\mathbf{d}}.
\end{aligned}$$

For the B_1 irrep in the moving frame with $|\mathbf{p}L/2\pi| = \sqrt{2}$, we choose $\mathbf{d} = \mathbf{p}L/2\pi = (1, 1, 0)$,

$$0 = \det \begin{pmatrix} -\cot \delta_0 + M_{21,21}^{B_1, \mathbf{p}} & M_{21,41}^{B_1, \mathbf{p}} & -M_{21,41}^{B_1, \mathbf{p}} \\ M_{21,41}^{B_1, \mathbf{p}} & -\cot \delta_4 + M_{41,41}^{B_1, \mathbf{p}} & M_{41,42}^{B_1, \mathbf{p}} \\ -M_{21,41}^{B_1, \mathbf{p}} & M_{41,42}^{B_1, \mathbf{p}} & -\cot \delta_4 + M_{41,41}^{B_1, \mathbf{p}} \end{pmatrix}, \quad (\text{B16})$$

where

$$\begin{aligned}
M_{21,21}^{B_1,\mathbf{p}} &= \omega_{00}^{\mathbf{d}} + \frac{5}{7}\omega_{20}^{\mathbf{d}} - \frac{12}{7}\omega_{40}^{\mathbf{d}} - i\frac{\sqrt{30}}{7}(\sqrt{5}\omega_{22}^{\mathbf{d}} + 2\sqrt{3}\omega_{42}^{\mathbf{d}}), \\
M_{21,41}^{B_1,\mathbf{p}} &= -\frac{5\sqrt{3}}{7}\omega_{20}^{\mathbf{d}} - \frac{15\sqrt{3}}{77}\omega_{40}^{\mathbf{d}} + \frac{10\sqrt{3}}{11}\omega_{60}^{\mathbf{d}} + \frac{5\sqrt{2}}{14}(-i + \sqrt{7})\omega_{22}^{\mathbf{d}} + \frac{3}{11}\sqrt{\frac{15}{14}}\left(5 + i\frac{9}{\sqrt{7}}\right)\omega_{42}^{\mathbf{d}} - \frac{4\sqrt{5}}{11}(1 - i\sqrt{7})\omega_{62}^{\mathbf{d}} \\
&\quad - i\frac{3\sqrt{30}}{11}\omega_{44}^{\mathbf{d}} - i\frac{10\sqrt{6}}{11}\omega_{64}^{\mathbf{d}}, \\
M_{41,41}^{B_1,\mathbf{p}} &= +\omega_{00}^{\mathbf{d}} + \frac{25}{77}\omega_{20}^{\mathbf{d}} - \frac{486}{1001}\omega_{40}^{\mathbf{d}} + \frac{8}{11}\omega_{60}^{\mathbf{d}} - \frac{224}{143}\omega_{80}^{\mathbf{d}} - i\frac{25\sqrt{6}}{77}\omega_{22}^{\mathbf{d}} - i\frac{243\sqrt{10}}{1001}\omega_{42}^{\mathbf{d}} - i\frac{\sqrt{105}}{11}\omega_{62}^{\mathbf{d}} - i\frac{42\sqrt{35}}{143}\omega_{82}^{\mathbf{d}} \\
&\quad + i\sqrt{\frac{21}{11}}\omega_{66}^{\mathbf{d}} + i14\sqrt{\frac{3}{143}}\omega_{86}^{\mathbf{d}}, \\
M_{41,42}^{B_1,\mathbf{p}} &= -\frac{60}{77}\omega_{20}^{\mathbf{d}} - \frac{1215}{1001}\omega_{40}^{\mathbf{d}} + \frac{9}{11}\omega_{60}^{\mathbf{d}} + \frac{168}{143}\omega_{80}^{\mathbf{d}} + \frac{5\sqrt{6}}{77}(3\sqrt{7} + i5)\omega_{22}^{\mathbf{d}} + \frac{81\sqrt{10}}{1001}(-\sqrt{7} + i3)\omega_{42}^{\mathbf{d}} + \frac{\sqrt{15}}{11}(-6 + i\sqrt{7})\omega_{62}^{\mathbf{d}} \\
&\quad + \frac{42\sqrt{5}}{143}(2 + i\sqrt{7})\omega_{82}^{\mathbf{d}} - i\frac{81\sqrt{10}}{143}\omega_{44}^{\mathbf{d}} - i\frac{3\sqrt{2}}{11}\omega_{64}^{\mathbf{d}} + i\frac{84}{13}\sqrt{\frac{2}{11}}\omega_{84}^{\mathbf{d}} + i\sqrt{\frac{21}{11}}\omega_{66}^{\mathbf{d}} + i14\sqrt{\frac{3}{143}}\omega_{86}^{\mathbf{d}}.
\end{aligned}$$

For the B_2 irrep in the moving frame with $|\mathbf{p}L/2\pi| = \sqrt{2}$, we choose $\mathbf{d} = \mathbf{p}L/2\pi = (1, 1, 0)$,

$$0 = \det \begin{pmatrix} -\cot \delta_0 + M_{21,21}^{B_2,\mathbf{p}} & M_{21,41}^{B_2,\mathbf{p}} & M_{21,41}^{B_2,\mathbf{p}} \\ M_{21,41}^{B_2,\mathbf{p}} & -\cot \delta_4 + M_{41,41}^{B_2,\mathbf{p}} & M_{41,42}^{B_2,\mathbf{p}} \\ M_{21,41}^{B_2,\mathbf{p}} & M_{41,42}^{B_2,\mathbf{p}} & -\cot \delta_4 + M_{41,41}^{B_2,\mathbf{p}} \end{pmatrix}, \quad (\text{B17})$$

where

$$\begin{aligned}
M_{21,21}^{B_2,\mathbf{p}} &= \omega_{00}^{\mathbf{d}} - \frac{10}{7}\omega_{20}^{\mathbf{d}} + \frac{3}{7}\omega_{40}^{\mathbf{d}} + 6\sqrt{\frac{5}{14}}\omega_{44}^{\mathbf{d}}, \\
M_{21,41}^{B_2,\mathbf{p}} &= -\frac{5\sqrt{6}}{14}\omega_{20}^{\mathbf{d}} + \frac{45\sqrt{6}}{77}\omega_{40}^{\mathbf{d}} - \frac{5\sqrt{6}}{22}\omega_{60}^{\mathbf{d}} - \frac{5}{\sqrt{7}}\omega_{22}^{\mathbf{d}} + \frac{6\sqrt{105}}{77}\omega_{42}^{\mathbf{d}} - \frac{\sqrt{10}}{22}\omega_{62}^{\mathbf{d}} + \frac{6\sqrt{105}}{77}\omega_{44}^{\mathbf{d}} - \frac{5\sqrt{21}}{11}\omega_{64}^{\mathbf{d}} - \frac{15}{\sqrt{22}}\omega_{66}^{\mathbf{d}}, \\
M_{41,41}^{B_2,\mathbf{p}} &= +\omega_{00}^{\mathbf{d}} - \frac{50}{77}\omega_{20}^{\mathbf{d}} + \frac{243}{2002}\omega_{40}^{\mathbf{d}} - \frac{13}{11}\omega_{60}^{\mathbf{d}} + \frac{203}{286}\omega_{80}^{\mathbf{d}} + \frac{243}{143}\sqrt{\frac{5}{14}}\omega_{44}^{\mathbf{d}} + \frac{3\sqrt{14}}{11}\omega_{64}^{\mathbf{d}} + \frac{42}{13}\sqrt{\frac{7}{22}}\omega_{84}^{\mathbf{d}} - 21\sqrt{\frac{5}{286}}\omega_{88}^{\mathbf{d}}, \\
M_{41,42}^{B_2,\mathbf{p}} &= +\frac{90}{77}\omega_{20}^{\mathbf{d}} - \frac{2025}{2002}\omega_{40}^{\mathbf{d}} - \frac{9}{11}\omega_{60}^{\mathbf{d}} + \frac{189}{286}\omega_{80}^{\mathbf{d}} + \frac{10}{11}\sqrt{\frac{6}{7}}\omega_{22}^{\mathbf{d}} - \frac{243}{143}\sqrt{\frac{10}{7}}\omega_{42}^{\mathbf{d}} + \frac{4\sqrt{5}}{11}\omega_{62}^{\mathbf{d}} - \frac{21\sqrt{5}}{143}\omega_{82}^{\mathbf{d}} + \frac{243}{143}\sqrt{\frac{5}{14}}\omega_{44}^{\mathbf{d}} \\
&\quad + \frac{3\sqrt{14}}{11}\omega_{64}^{\mathbf{d}} + \frac{42}{13}\sqrt{\frac{7}{22}}\omega_{84}^{\mathbf{d}} + 4\sqrt{\frac{3}{11}}\omega_{66}^{\mathbf{d}} - 7\sqrt{\frac{21}{143}}\omega_{86}^{\mathbf{d}} + 21\sqrt{\frac{5}{286}}\omega_{88}^{\mathbf{d}}.
\end{aligned}$$

For the A_1 irrep in the moving frame with $|\mathbf{p}L/2\pi| = \sqrt{3}$, we choose $\mathbf{d} = \mathbf{p}L/2\pi = (1, 1, 1)$,

$$0 = \det \begin{pmatrix} -\cot \delta_0 + \omega_{00}^{\mathbf{d}} & \sqrt{30}\omega_{22}^{\mathbf{d}} & \frac{6\sqrt{21}}{7}\omega_{40}^{\mathbf{d}} & 3\sqrt{3}(1 - i)\omega_{42}^{\mathbf{d}} \\ -\sqrt{30}\omega_{22}^{\mathbf{d}} & -\cot \delta_2 + M_{21,21}^{A_1,\mathbf{p}} & M_{21,41}^{A_1,\mathbf{p}} & M_{21,42}^{A_1,\mathbf{p}} \\ \frac{6\sqrt{21}}{7}\omega_{40}^{\mathbf{d}} & M_{21,41}^{A_1,\mathbf{p}} & M_{41,41}^{A_1,\mathbf{p}} - \cot \delta_2 & M_{41,42}^{A_1,\mathbf{p}} \\ 3\sqrt{3}(-1 - i)\omega_{42}^{\mathbf{d}} & M_{21,42}^{A_1,\mathbf{p}} & M_{41,42}^{A_1,\mathbf{p}} & M_{42,42}^{A_1,\mathbf{p}} - \cot \delta_4 \end{pmatrix}, \quad (\text{B18})$$

where

$$\begin{aligned}
M_{21,21}^{A_1,\mathbf{p}} &= \omega_{00}^{\mathbf{d}} - \frac{12}{7}\omega_{40}^{\mathbf{d}} - i\frac{10\sqrt{6}}{7}\omega_{22}^{\mathbf{d}} - i\frac{12\sqrt{10}}{7}\omega_{42}^{\mathbf{d}}, \\
M_{21,41}^{A_1,\mathbf{p}} &= +2\sqrt{\frac{10}{7}}\omega_{22}^{\mathbf{d}} + \frac{30}{11}\sqrt{\frac{6}{7}}\omega_{42}^{\mathbf{d}} - \frac{260}{99}(1-i)\omega_{63}^{\mathbf{d}} - \frac{100}{9}\sqrt{\frac{5}{11}}\omega_{66}^{\mathbf{d}}, \\
M_{21,42}^{A_1,\mathbf{p}} &= -\frac{20}{77}(1+i)\omega_{22}^{\mathbf{d}} - \frac{30\sqrt{6}}{77}(1-i)\omega_{40}^{\mathbf{d}} - \frac{39\sqrt{15}}{77}(1+i)\omega_{42}^{\mathbf{d}} + \frac{20\sqrt{6}}{11}(1-i)\omega_{60}^{\mathbf{d}} + \frac{64\sqrt{70}}{99}\omega_{63}^{\mathbf{d}} + \frac{20}{9}\sqrt{\frac{14}{11}}(1+i)\omega_{66}^{\mathbf{d}}, \\
M_{41,41}^{A_1,\mathbf{p}} &= \omega_{00}^{\mathbf{d}} + \frac{324}{143}\omega_{40}^{\mathbf{d}} + \frac{80}{11}\omega_{60}^{\mathbf{d}} + \frac{560}{143}\omega_{80}^{\mathbf{d}}, \\
M_{41,42}^{A_1,\mathbf{p}} &= -\frac{10}{11}\sqrt{\frac{15}{7}}(1-i)\omega_{22}^{\mathbf{d}} - \frac{81}{11}\sqrt{\frac{1}{7}}(1-i)\omega_{42}^{\mathbf{d}} - i\frac{80}{33}\sqrt{\frac{2}{3}}\omega_{63}^{\mathbf{d}} - \frac{4}{3}\sqrt{\frac{10}{33}}(1-i)\omega_{66}^{\mathbf{d}} + \frac{8}{11}\sqrt{\frac{210}{143}}(1-i)\omega_{86}^{\mathbf{d}} + i\frac{240}{11}\sqrt{\frac{7}{143}}\omega_{87}^{\mathbf{d}}, \\
M_{42,42}^{A_1,\mathbf{p}} &= \omega_{00}^{\mathbf{d}} - \frac{162}{77}\omega_{40}^{\mathbf{d}} + \frac{20}{11}\omega_{60}^{\mathbf{d}} - i\frac{65\sqrt{6}}{77}\omega_{22}^{\mathbf{d}} + i\frac{162\sqrt{10}}{1001}\omega_{42}^{\mathbf{d}} + \frac{20}{33}\sqrt{\frac{35}{3}}(1+i)\omega_{63}^{\mathbf{d}} + i\frac{4}{3}\sqrt{\frac{77}{3}}\omega_{66}^{\mathbf{d}} \\
&\quad + i\frac{7952}{143}\sqrt{\frac{3}{143}}\omega_{86}^{\mathbf{d}} + \frac{1008}{143}\sqrt{\frac{10}{143}}(1+i)\omega_{87}^{\mathbf{d}}.
\end{aligned}$$

For the E irrep in the moving frame with $|\mathbf{p}L/2\pi| = \sqrt{3}$, we choose $\mathbf{d} = \mathbf{p}L/2\pi = (1, 1, 1)$,

$$0 = \det \begin{pmatrix} -\cot\delta_2 + M_{21,21}^{E,\mathbf{p}} & M_{21,22}^{E,\mathbf{p}} & M_{21,41}^{E,\mathbf{p}} & M_{21,42}^{E,\mathbf{p}} & M_{21,43}^{E,\mathbf{p}} \\ M_{21,22}^{E,\mathbf{p}} & -\cot\delta_2 + M_{22,22}^{E,\mathbf{p}} & M_{22,41}^{E,\mathbf{p}} & M_{22,42}^{E,\mathbf{p}} & M_{22,43}^{E,\mathbf{p}} \\ M_{21,41}^{E,\mathbf{p}} & M_{22,41}^{E,\mathbf{p}} & -\cot\delta_4 + M_{41,41}^{E,\mathbf{p}} & M_{41,42}^{E,\mathbf{p}} & M_{41,43}^{E,\mathbf{p}} \\ M_{21,42}^{E,\mathbf{p}} & M_{22,42}^{E,\mathbf{p}} & M_{41,42}^{E,\mathbf{p}} & -\cot\delta_4 + M_{42,42}^{E,\mathbf{p}} & M_{42,43}^{E,\mathbf{p}} \\ M_{21,43}^{E,\mathbf{p}} & M_{22,43}^{E,\mathbf{p}} & M_{41,43}^{E,\mathbf{p}} & M_{42,43}^{E,\mathbf{p}} & -\cot\delta_4 + M_{43,43}^{E,\mathbf{p}} \end{pmatrix},$$

where

$$\begin{aligned}
M_{21,21}^{E,\mathbf{p}} &= \omega_{00}^{\mathbf{d}} + \frac{18}{7}\omega_{40}^{\mathbf{d}}, \\
M_{21,22}^{E,\mathbf{p}} &= \frac{\sqrt{10}}{14}(1-i)(\sqrt{60}\omega_{22}^{\mathbf{d}} - 9\omega_{42}^{\mathbf{d}}), \\
M_{21,41}^{E,\mathbf{p}} &= +\frac{15\sqrt{2}}{14}(1-i)\omega_{22}^{\mathbf{d}} + \frac{12\sqrt{30}}{77}(1-i)\omega_{42}^{\mathbf{d}} - i\frac{32\sqrt{35}}{33}\omega_{63}^{\mathbf{d}} + \frac{10}{3}\sqrt{\frac{7}{11}}(1-i)\omega_{66}^{\mathbf{d}}, \\
M_{21,42}^{E,\mathbf{p}} &= \frac{30\sqrt{3}}{77}(-4\omega_{40}^{\mathbf{d}} - 7\omega_{60}^{\mathbf{d}}), \\
M_{21,43}^{E,\mathbf{p}} &= -\frac{5\sqrt{21}}{7}\omega_{22}^{\mathbf{d}} + \frac{18\sqrt{35}}{77}\omega_{42}^{\mathbf{d}} - \frac{4}{33}\sqrt{\frac{10}{3}}(1-i)\omega_{63}^{\mathbf{d}} - \frac{70}{3}\sqrt{\frac{2}{33}}\omega_{66}^{\mathbf{d}}, \\
M_{22,22}^{E,\mathbf{p}} &= \omega_{00}^{\mathbf{d}} + i\frac{5\sqrt{6}}{7}\omega_{22}^{\mathbf{d}} - \frac{12}{7}\omega_{40}^{\mathbf{d}} + i\frac{6\sqrt{10}}{7}\omega_{42}^{\mathbf{d}}, \\
M_{22,41}^{E,\mathbf{p}} &= -i\frac{10\sqrt{2}}{7}\omega_{22}^{\mathbf{d}} + \frac{60\sqrt{3}}{77}\omega_{40}^{\mathbf{d}} - i\frac{39\sqrt{30}}{154}\omega_{42}^{\mathbf{d}} - \frac{40\sqrt{3}}{11}\omega_{60}^{\mathbf{d}} + i\frac{32\sqrt{35}}{99}(1+i)\omega_{63}^{\mathbf{d}} + i\frac{20\sqrt{77}}{99}\omega_{66}^{\mathbf{d}}, \\
M_{22,42}^{E,\mathbf{p}} &= -\frac{10\sqrt{2}}{7}(1+i)\omega_{22}^{\mathbf{d}} + \frac{3\sqrt{30}}{7}(1+i)\omega_{42}^{\mathbf{d}} - \frac{4\sqrt{35}}{9}\omega_{63}^{\mathbf{d}} + i\frac{20}{9}\sqrt{\frac{7}{11}}(1+i)\omega_{66}^{\mathbf{d}}, \\
M_{22,43}^{E,\mathbf{p}} &= -\frac{9\sqrt{35}}{22}(1-i)\omega_{42}^{\mathbf{d}} + i\frac{32}{11}\sqrt{\frac{10}{3}}\omega_{63}^{\mathbf{d}} - 10\sqrt{\frac{2}{33}}(1-i)\omega_{66}^{\mathbf{d}},
\end{aligned}$$

$$\begin{aligned}
M_{41,41}^{E,p} &= \omega_{00}^d - \frac{162}{77} \omega_{40}^d + \frac{20}{11} \omega_{60}^d + i \frac{65\sqrt{6}}{154} \omega_{22}^d - i \frac{81\sqrt{10}}{1001} \omega_{42}^d - \frac{10}{33} \sqrt{\frac{35}{3}} (1+i) \omega_{63}^d - i \frac{2}{3} \sqrt{\frac{77}{3}} \omega_{66}^d \\
&\quad - i \frac{3976}{143} \sqrt{\frac{3}{143}} \omega_{86}^d - \frac{504}{143} \sqrt{\frac{10}{143}} (1+i) \omega_{87}^d, \\
M_{41,42}^{E,p} &= -\frac{5\sqrt{6}}{7} (1+i) \omega_{22}^d + \frac{405\sqrt{10}}{2002} (1+i) \omega_{42}^d - \frac{16}{33} \sqrt{\frac{35}{3}} \omega_{63}^d + \frac{4}{3} \sqrt{\frac{7}{33}} (1+i) \omega_{66}^d - \frac{238}{13} \sqrt{\frac{3}{143}} (1+i) \omega_{86}^d - \frac{168}{13} \sqrt{\frac{10}{143}} \omega_{87}^d, \\
M_{41,43}^{E,p} &= -\frac{15\sqrt{7}}{22} (1-i) \omega_{22}^d - i \frac{2\sqrt{10}}{3} \omega_{63}^d - \frac{\sqrt{22}}{33} (1-i) \omega_{66}^d - \frac{24}{11} \sqrt{\frac{14}{143}} (1-i) \omega_{86}^d - i \frac{48}{11} \sqrt{\frac{105}{143}} \omega_{87}^d, \\
M_{42,42}^{E,p} &= \omega_{00}^d + \frac{324}{1001} \omega_{40}^d - \frac{64}{11} \omega_{60}^d + \frac{392}{143} \omega_{80}^d, \\
M_{42,43}^{E,p} &= +\frac{30\sqrt{7}}{77} \omega_{22}^d - \frac{243}{143} \sqrt{\frac{15}{7}} \omega_{42}^d + \frac{16\sqrt{10}}{33} (1-i) \omega_{63}^d + \frac{28}{3} \sqrt{\frac{2}{11}} \omega_{66}^d - \frac{1434}{143} \sqrt{\frac{14}{143}} \omega_{86}^d + \frac{48}{143} \sqrt{\frac{105}{143}} (1-i) \omega_{87}^d, \\
M_{43,43}^{E,p} &= \omega_{00}^d + \frac{162}{143} \omega_{40}^d - \frac{4}{11} \omega_{60}^d - \frac{448}{143} \omega_{80}^d - i \frac{5\sqrt{6}}{22} \omega_{22}^d - i \frac{81\sqrt{10}}{143} \omega_{42}^d - \frac{26}{33} \sqrt{\frac{35}{3}} (1+i) \omega_{63}^d - i \frac{14}{3} \sqrt{\frac{7}{33}} \omega_{66}^d \\
&\quad + i \frac{1288}{143} \sqrt{\frac{3}{143}} \omega_{86}^d + \frac{840}{143} \sqrt{\frac{10}{143}} (1+i) \omega_{87}^d.
\end{aligned}$$

-
- [1] C. Liu, Proc. Sci. LATTICE2016 (2017) 006 [arXiv:1612.00103].
- [2] R. A. Briceño, J. J. Dudek, and R. D. Young, *Rev. Mod. Phys.* **90**, 025001 (2018).
- [3] M. Padmanath, Proc. Sci. LATTICE2018 (2018) 013 [arXiv:1905.09651].
- [4] J. J. Dudek, R. G. Edwards, and C. E. Thomas (Hadron Spectrum Collaboration), *Phys. Rev. D* **87**, 034505 (2013); **90**, 099902(E) (2014).
- [5] J. J. Dudek, R. G. Edwards, M. J. Peardon, D. G. Richards, and C. E. Thomas, *Phys. Rev. D* **83**, 071504 (2011).
- [6] J. J. Dudek, R. G. Edwards, and C. E. Thomas, *Phys. Rev. D* **86**, 034031 (2012).
- [7] S. R. Beane, E. Chang, W. Detmold, H. W. Lin, T. C. Luu, K. Orginos, A. Parreño, M. J. Savage, A. Torok, and A. Walker-Loud (NPLQCD Collaboration), *Phys. Rev. D* **85**, 034505 (2012).
- [8] J. Bulava, B. Fahy, B. Hörz, K. J. Juge, C. Morningstar, and C. H. Wong, *Nucl. Phys.* **B910**, 842 (2016).
- [9] C. Michael, *Nucl. Phys.* **B259**, 58 (1985).
- [10] M. Lüscher and U. Wolff, *Nucl. Phys.* **B339**, 222 (1990).
- [11] B. Blossier, M. Della Morte, G. von Hippel, T. Mendes, and R. Sommer, *J. High Energy Phys.* **04** (2009) 094.
- [12] M. S. Mahbub, A. Ó. Cais, W. Kamleh, B. G. Lasscock, D. B. Leinweber, and A. G. Williams, *Phys. Rev. D* **80**, 054507 (2009).
- [13] R. J. Hudspith, B. Colquhoun, A. Francis, R. Lewis, and K. Maltman, *Phys. Rev. D* **102**, 114506 (2020).
- [14] Y. Chen *et al.*, *Phys. Rev. D* **89**, 094506 (2014).
- [15] P. Adlarson *et al.* (WASA-at-COSY Collaboration), *Phys. Rev. Lett.* **106**, 242302 (2011).
- [16] P. Adlarson *et al.* (WASA-at-COSY Collaboration), *Phys. Rev. Lett.* **112**, 202301 (2014).
- [17] H. Witała and W. Glöckle, *Nucl. Phys.* **A528**, 48 (1991).
- [18] W. Tornow, H. Witała, and A. Kievsky, *Phys. Rev. C* **57**, 555 (1998).
- [19] D. Huber and J. L. Friar, *Phys. Rev. C* **58**, 674 (1998).
- [20] A. V. Anisovich, V. V. Anisovich, and A. V. Sarantsev, *Phys. Rev. D* **62**, 051502 (2000).
- [21] D. Ebert, R. N. Faustov, and V. O. Galkin, *Phys. Rev. D* **79**, 114029 (2009).
- [22] H. B. Meyer and M. J. Teper, *Phys. Lett. B* **605**, 344 (2005).
- [23] M. T. Hansen and S. R. Sharpe, *Annu. Rev. Nucl. Part. Sci.* **69**, 65 (2019).
- [24] M. Mai, M. Döring, and A. Rusetsky, *Eur. Phys. J. Spec. Top.* **230**, 1623 (2021).
- [25] C. T. Johnson and J. J. Dudek (Hadron Spectrum Collaboration), *Phys. Rev. D* **103**, 074502 (2021).
- [26] M. Lüscher, *Nucl. Phys.* **B354**, 531 (1991).
- [27] M. Lüscher, *Commun. Math. Phys.* **105**, 153 (1986).
- [28] K. Rummukainen and S. A. Gottlieb, *Nucl. Phys.* **B450**, 397 (1995).
- [29] C. h. Kim, C. T. Sachrajda, and S. R. Sharpe, *Nucl. Phys.* **B727**, 218 (2005).
- [30] Z. Fu, *Phys. Rev. D* **85**, 014506 (2012).
- [31] M. Göckeler, R. Horsley, M. Lage, U. G. Meißner, P. E. L. Rakow, A. Rusetsky, G. Schierholz, and J. M. Zanotti, *Phys. Rev. D* **86**, 094513 (2012).

- [32] P. Guo, J. Dudek, R. Edwards, and A. P. Szczepaniak, *Phys. Rev. D* **88**, 014501 (2013).
- [33] T. Luu and M. J. Savage, *Phys. Rev. D* **83**, 114508 (2011).
- [34] L. Leskovec and S. Prelovsek, *Phys. Rev. D* **85**, 114507 (2012).
- [35] R. A. Briceño and Z. Davoudi, *Phys. Rev. D* **88**, 094507 (2013).
- [36] R. A. Briceño, *Phys. Rev. D* **89**, 074507 (2014).
- [37] E. Berkowitz, T. Kurth, A. Nicholson, B. Joo, E. Rinaldi, M. Strother, P. M. Vranas, and A. Walker-Loud, *Phys. Lett. B* **765**, 285 (2017).
- [38] J.-J. Wu, T.-S. H. Lee, D. B. Leinweber, A. W. Thomas, and R. D. Young, *J. Phys. Soc. Jpn. Conf. Proc.* **10**, 062002 (2016).
- [39] Y. Li, J.-J. Wu, C. D. Abell, D. B. Leinweber, and A. W. Thomas, *Phys. Rev. D* **101**, 114501 (2020).
- [40] Y. Li, J.-J. Wu, D. B. Leinweber, and A. W. Thomas, *Phys. Rev. D* **103**, 094518 (2021).
- [41] S. Amarasinghe, R. Baghdadi, Z. Davoudi, W. Detmold, M. Illa, A. Parreño, A. V. Pochinsky, P. E. Shanahan, and M. L. Wagman, [arXiv:2108.10835](https://arxiv.org/abs/2108.10835).
- [42] M. Weissbluth, *Atoms and Molecules* (Elsevier Science, New York, 2012).
- [43] M. Döring, U. Meißner, E. Oset, and A. Rusetsky, *Eur. Phys. J. A* **48**, 114 (2012).
- [44] G. S. Bali *et al.*, *Nucl. Phys.* **B866**, 1 (2013).
- [45] X. Feng, K. Jansen, and D. B. Renner, *Phys. Lett. B* **684**, 268 (2010).
- [46] W. Detmold and B. Smigielski, *Proc. Sci. LATTICE2010* (**2010**) 100 [[arXiv:1101.2639](https://arxiv.org/abs/1101.2639)].
- [47] W. Detmold and B. Smigielski, *Phys. Rev. D* **84**, 014508 (2011).
- [48] W. Detmold, K. Orginos, and Z. Shi, *Phys. Rev. D* **86**, 054507 (2012).
- [49] C. Culver, M. Mai, A. Alexandru, M. Döring, and F. X. Lee, *Phys. Rev. D* **100**, 034509 (2019).
- [50] C. Culver, M. Mai, R. Brett, A. Alexandru, and M. Döring, *Phys. Rev. D* **101**, 114507 (2020).
- [51] M. S. Mahbub, W. Kamleh, D. B. Leinweber, P. J. Moran, and A. G. Williams, *Phys. Rev. D* **87**, 094506 (2013).
- [52] F. M. Stokes, W. Kamleh, D. B. Leinweber, M. S. Mahbub, B. J. Menadue, and B. J. Owen, *Phys. Rev. D* **92**, 114506 (2015).
- [53] S. R. Beane, T. C. Luu, K. Orginos, A. Parreño, M. J. Savage, A. Torok, and A. Walker-Loud, *Phys. Rev. D* **77**, 014505 (2008).
- [54] S. R. Beane, W. Detmold, T. C. Luu, K. Orginos, A. Parreño, M. J. Savage, A. Torok, and A. Walker-Loud, *Phys. Rev. D* **79**, 114502 (2009).
- [55] R. G. Edwards and B. Joo (SciDAC, LHPC, UKQCD Collaborations), *Nucl. Phys. B, Proc. Suppl.* **140**, 832 (2005).